

Macrophages induce inflammation by efferocytosis of apoptotic prostate cancer cells via HIF-1 α stabilization

Veronica Mendoza-Reinoso^{1,†}, Patricia M. Schnepf^{2,†}, Dah Youn Baek¹, John R. Rubin¹, Ernestina Schipani³, Evan T. Keller^{2*}, Laurie K. McCauley^{1*}, Hernan Roca^{1*}

*For correspondence:

rocach@umich.edu

mccauley@umich.edu

etkeller@med.umich.edu

¹Department of Periodontics and Oral Medicine, University of Michigan School of Dentistry, Ann Arbor, United States;

²Department of Urology, Medical School, University of Michigan, Ann Arbor, United States; ³Department of Orthopaedic Surgery, School of Medicine, University of Pennsylvania, Philadelphia, United States.

[†] These authors contributed equally to this work.

Abstract

Clearance of apoptotic cancer cells by macrophages, known as efferocytosis, fuels the bone-metastatic growth of prostate cancer cells via pro-inflammatory and immunosuppressive processes. However, the exact molecular mechanisms remain unclear. In this study, single-cell transcriptomics of bone marrow macrophages undergoing efferocytosis of apoptotic prostate cancer cells revealed a significant enrichment of a cellular response to hypoxia. Here we show that efferocytic macrophages promote HIF-1 α stabilization under normoxic conditions through interaction with phosphorylated STAT3. Inflammatory cytokine gene expression analysis of efferocytic HIF-1 α -mutant macrophages revealed a reduced expression of the pro-tumorigenic *Mif*. Furthermore, stabilization of HIF-1 α using the HIF-prolyl-hydroxylase inhibitor, Roxadustat, enhanced MIF expression in macrophages. Finally,

29 macrophages treated with recombinant MIF protein activated NF- κ B (p65) signaling and increased the expression of pro-
30 inflammatory cytokines. Altogether, these findings suggest that the clearance of apoptotic cancer cells by tumor-associated
31 macrophages triggers p-STAT3/HIF-1 α /MIF signaling to enhance tumor-promoting inflammation in bone, suggesting this axis as
32 a target for metastatic prostate cancer.

34 Introduction

35
36 The process of clearing of apoptotic cancer cells by macrophages, known as efferocytosis, commonly occurs during tumor
37 progression and fuels the bone-metastatic growth of cancer cells, via subsequent pro-inflammatory and immunosuppressive
38 activity (Graham *et al*, 2014; Lecoultre *et al*, 2020; Roca & McCauley, 2018; Stanford *et al*, 2014). Our previous published work
39 reported that bone marrow macrophage-dependent efferocytosis of apoptotic prostate cancer cells supported skeletal tumor
40 growth through the secretion of pro-inflammatory cytokines resulting in an immunosuppressive response (Mendoza-Reinoso *et*
41 *al*, 2020; Roca *et al*, 2018). Recently, a single-cell RNA sequencing study reported that peritoneal macrophage efferocytosis of
42 apoptotic T cells displayed a heterogeneous transcriptional activity including genes associated with predisposition for
43 efferocytosis, macrophage differentiation, locomotion and inflammation (Lantz *et al*, 2020). However, the precise molecular
44 mechanisms involved in bone marrow macrophage response to efferocytosis of apoptotic cancer cells remains to be elucidated.

45
46 The majority of solid tumors present areas of permanent or transient hypoxia due to poor vascularization and blood supply
47 (Pouyssegur *et al*, 2006). Hypoxic conditions activate hypoxia inducible factor (HIF) signaling which has a crucial role in pro-
48 tumorigenic inflammatory processes via cytokine secretion, reactive oxygen species (ROS) production and angiogenesis (Triner &
49 Shah, 2016). HIFs are heterodimers consisting of an oxygen labile alpha (α) subunit and a stable beta (β) subunit. There are
50 three isoforms of HIF- α , including HIF-1 α , HIF-2 α (EPAS1) and HIF-3 α (IPAS) (Kaelin & Ratcliffe, 2008). HIF-1 α upregulates
51 glycolytic genes such as phosphoglycerate kinase (PGK) and lactate dehydrogenase A (LDHA) whereas HIF-2 α induces the
52 expression of genes related to oxygen supply improvement in hypoxic regions such as erythropoietin (EPO) (Hu *et al*, 2003). HIF-
53 1 α has been identified as a key regulator of proliferative, invasive and immunosuppressive mechanisms that favor tumor
54 progression (Engel *et al*, 2017; Hatfield *et al*, 2019). Under hypoxic conditions, HIF-1 α hydroxylation by prolyl hydroxylase is
55 reduced. This inhibits the HIF-1 α /Von Hippel-Lindau (VHL) interaction and consequent HIF-1 α degradation by ubiquitin E3 ligase
56 complex (Jaakkola *et al*, 2001). Therefore, HIF-1 α is stabilized in the cytosol and translocated to the nucleus to promote the
57 transcription of multiple target genes (Semenza, 2011). HIF-1 α is strikingly upregulated under hypoxic conditions, however, HIF-
58 1 α can also be regulated at transcriptional, translational and post-translational levels under normoxic conditions (Hayashi *et al*,
59 2019). HIF-1 α is expressed and stabilized in immune cells via hypoxia or other factors such as inflammation, cancer and
60 infectious microorganisms (Blouin *et al*, 2004; Hartmann *et al*, 2008; Peyssonnaud *et al*, 2005). HIF-1 α is crucial for myeloid cell-
61 mediated inflammation (Cramer *et al*, 2003) and it has been demonstrated that tumor-associated macrophages (TAMs) also

62 express HIF-2 α under hypoxic conditions (Imtiyaz *et al*, 2010; Talks *et al*, 2000). Various studies have shown a relationship
63 between HIF-1 α induction and STAT3 activation at post-translational and transcriptional levels (Gray *et al*, 2005; Jung *et al*,
64 2008; Niu *et al*, 2008; Xu *et al*, 2005).

65
66 Previous reports have shown that low oxygen concentrations in tumors promote the secretion of cytokines and chemokines that
67 recruit pro-tumorigenic Tregs, tumor-associated macrophages, neutrophils, B cells, and myeloid-derived suppressor cells
68 (MDSCs) to support tumor growth (Blaisdell *et al*, 2015; Du *et al*, 2008; Facciabene *et al*, 2011; Zhu *et al*, 2014). One of these
69 cytokines is macrophage migration factor (MIF), which is a direct target gene of HIF-1 α (Winner *et al*, 2007) and a hypoxia-
70 induced gene in colon and breast cancer cells (Larsen *et al*, 2008; Yao *et al*, 2005). MIF acts as an autocrine or paracrine
71 cytokine, it is upregulated in several types of cancer (Mawhinney *et al*, 2015; Tomiyasu *et al*, 2002; Wilson *et al*, 2005) and its
72 expression correlates with disease malignancy and invasiveness (Lippitz, 2013). Studies consistently demonstrated that MIF
73 signals primarily through CD74 in association with CD44, CXCR2, CXCR4, and CXCR7 to activate the ERK MAP kinase cascade
74 (Leng *et al*, 2003; Shi *et al*, 2006; Tarnowski *et al*, 2010). Finally, MIF signaling induces the activation and secretion of pro-
75 tumorigenic cytokines to support tumor growth (Bach *et al*, 2008; Bucala & Donnelly, 2007) .

76
77 Using single-cell transcriptomic sequencing, we investigated the signature changes in bone marrow macrophage gene expression
78 during efferocytosis of apoptotic prostate cancer cells. We found that macrophages engulfing apoptotic prostate cancer cells
79 promoted HIF-1 α stability by its interaction with phosphorylated STAT3 and induced the expression of the pro-inflammatory
80 cytokine MIF. Thus, p-STAT3/HIF1 α /MIF signaling in tumor-associated macrophages may have a pro-tumorigenic effect in the bone
81 marrow tumor microenvironment that contributes to skeletal metastasis and can be used to target preventive and therapeutic
82 approaches.

83 **Results**

84 ***Single cell analyses of macrophages engulfing apoptotic prostate cancer cells show a distinct transcriptional signature*** 85 ***and the activation of hypoxia-related genes.***

86
87
88 Published findings suggest that macrophages induce distinctive tumor-promoting signaling in response to efferocytosis of
89 apoptotic cancer cells (Mendoza-Reinoso *et al*, 2020; Roca *et al*, 2018; Soki *et al*, 2014; Stanford *et al*, 2014). However, the
90 mechanisms that govern these specific responses in connection to tumor acceleration are not completely understood. To further
91 investigate the efferocytosis-mediated signaling in bone macrophages, primary bone marrow macrophages from
92 immunocompetent C57BL/6J mice were co-cultured with CFSE⁺ (pre-labeled) apoptotic prostate cancer RM1 cells. Macrophages
93 engulfing these apoptotic cancer cells (efferocytic) were compared to non-engulfing (non-efferocytic) macrophages by single-cell
94 RNA sequencing upon sorting by flow cytometry (Figure 1A). After identification of high quality sequenced single cells (Table 1,

95 Supplementary data), UMAP (Becht *et al*, 2018) was applied for dimension reduction of single cell analysis and visualization of
96 the transcriptional data for efferocytic and non-efferocytic macrophages. As shown in Figure 1B the cell distribution in two UMAP
97 projections depicts different cluster enrichment in efferocytic vs. non-efferocytic macrophages from two independent
98 experiments (Exp. 1 and Exp. 2). For example, efferocytic cells demonstrate enriched in cluster in the direction of increased
99 UMAP-2-projection while the opposite is observed in non-efferocytic macrophages as shown in the split visualization of these
100 cells (Figure 1B). These results correlate with distinct transcriptional heatmaps in efferocytic relative to non-efferocytic
101 macrophages (Figure 1C) where the great majority of differentially expressed genes (DEG's) significantly changed in the same
102 direction (3277 vs 482) in both experiments as analyzed in the Venn diagram in Figure 1D. DEG's commonly upregulated in
103 efferocytic macrophages in both experiments were further processed using the PANTHER analysis (Mi *et al*, 2013; Thomas *et al*,
104 2003) and gene ontology database (Ashburner *et al*, 2000; Gene Ontology, 2021) to identify the relevant biological pathways.
105 Among the significantly enriched GO- biological processes identified we found pathways related to the innate immune system
106 and wound healing responses which are related to phagocytosis of apoptotic cells, inflammation, and regeneration (Figure 1E,
107 list of enriched GO terms in Table 1, Supplementary data) (Koh & DiPietro, 2011; Minutti *et al*, 2017). Intriguingly, biological
108 processes related to hypoxia were identified even though these experiments were performed under normoxia (normal oxygen
109 conditions), which suggests that efferocytosis mediated activation and upregulation of factors directly related to cellular hypoxia
110 is independent of the oxygen concentration (Figure 1E and Figure 1F).

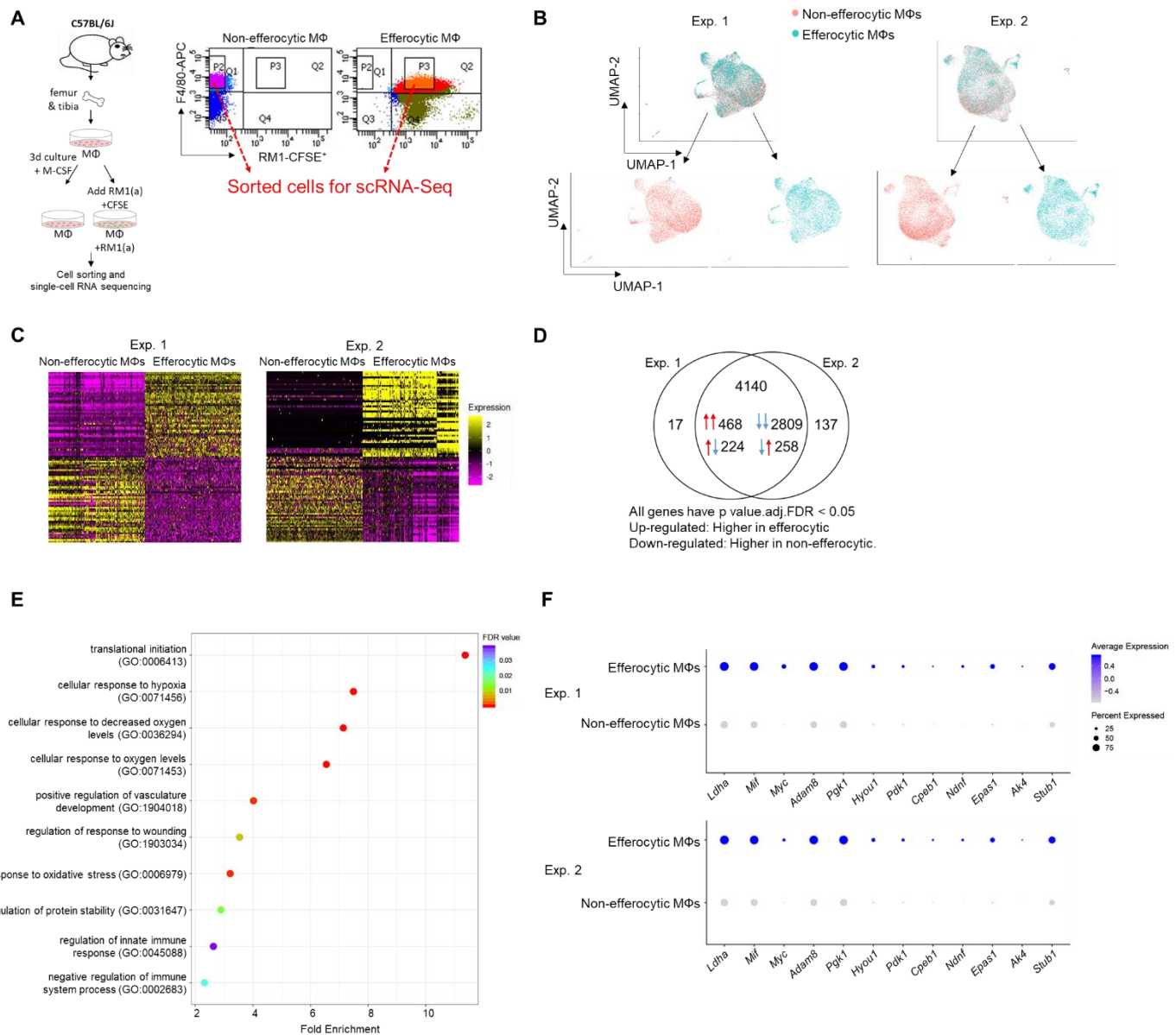


Figure 1. Single-cell experiments comparing efferocytic macrophages (engulfing apoptotic cancer cells) vs control (non-engulfing macrophages)

A. Bone marrow-derived macrophages were isolated from 4 week old C57BL/6J mice and co-cultured with apoptotic RM1(a) cells for 16-18 hours. Efferocytic ($F4/80^+CFSE^+$) and control macrophages ($F4/80^+$) were sorted and used for single-cell libraries followed by single-cell RNA sequencing. **B.** UMAP of all cells, blue represents efferocytic macrophages and red represents non-efferocytic macrophages. **C.** Heatmap of top differential expressed genes in either experiment. **D.** Venn Diagram of overlap of all differentially expressed genes between both experiments. **E.** Cleveland plot of top enrichment pathways in efferocytic macrophages. **F.** Dot plots of hypoxia-related genes in both experiments. Size relates to the percentage of macrophage cells that expressed each gene. Color denotes the average expression for each gene across all expressing cells. Additional results are shown in Supplementary data – Table 1, 2 and 3.

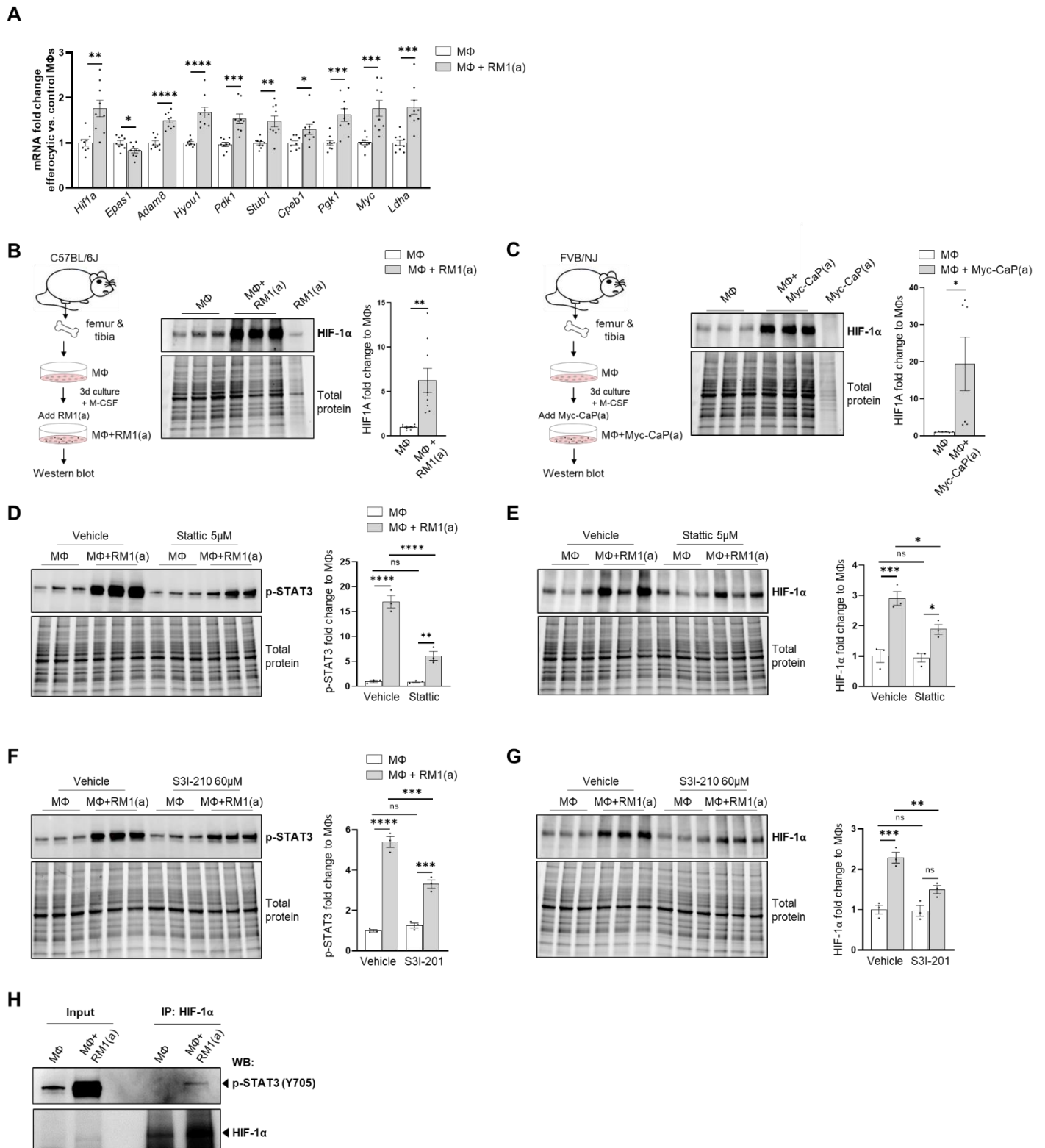
125 ***Efferocytosis of apoptotic cancer cells stabilizes HIF-1 α in bone macrophages which is mediated by the activation of***
126 ***STAT3.***

127 Single cell analysis of efferocytic macrophages identified upregulated molecules associated with gene ontology (GO) term of cellular
128 hypoxia (Figure 1). To investigate these findings in the overall macrophage population, co-cultures of bone macrophages with apoptotic
129 prostate cancer RM1 cells (workflow Figure 1A) were analyzed. Selected hypoxia-GO associated genes showing significant upregulation
130 by sc-RNAseq were investigated by RT-qPCR from total RNA isolated from co-cultures of independent bone macrophage populations.
131 Fold changes in efferocytic relative to control macrophages were calculated and plotted in Figure 2A. The majority of analyzed genes
132 showed a significant mRNA increase in efferocytic macrophages relative to control in correlation with the single cell results. Some of
133 these molecules are crucial components of glycolysis including *Pdk1*, *Pgk1*, and *Ldha* and are known targets of hypoxia inducible factor
134 1 α (HIF-1 α), a master transcriptional regulator of cellular response to hypoxia that promotes metabolic switch to glycolysis (Niu *et al.*,
135 2008; Palazon *et al.*, 2014). *Hif1a* was upregulated in the overall population of efferocytic macrophages (although it was not identified
136 as an upregulated gene in the single-cell experiments). Contrary to the results observed by single-cell experiments, the hypoxia-
137 inducible transcription factor *Epas1* (HIF-2 α) (Imtiyaz *et al.*, 2010) showed a small but significant decrease in mRNA expression by
138 efferocytosis.

139
140 Because HIF-1 α is largely regulated post-transcriptionally resulting in a protein targeted for degradation under normoxic conditions
141 (Ivan *et al.*, 2001; Jaakkola *et al.*, 2001), HIF-1 α protein was further evaluated by Western blot. As shown in Figure 2B, Western blot
142 analysis of efferocytic macrophages (co-cultured for 16-18 hours with apoptotic RM1 cells) evidenced a significant increase of HIF-1 α
143 induced by efferocytosis. These findings were further corroborated in efferocytic bone marrow derived macrophages co-cultured with
144 murine prostate cancer Myc-CaP cells, which share several molecular characteristics of human prostate cancer (Dudzinski *et al.*, 2019;
145 Ellwood-Yen *et al.*, 2003). As Myc-CaP cancer cells were obtained from FVB/NJ mice, the primary macrophages were obtained from the
146 bone marrow of the same strain. Similar results were observed using this model (Figure 2C). These results suggest that HIF-1 α is
147 stabilized in macrophages engulfing apoptotic cancer cells.

148
149 The potential mechanism inducing HIF-1 α stabilization was further investigated. Previous findings suggested that one potential
150 mechanism leading to HIF-1 α stabilization is via interaction with activated (phosphorylated) STAT3 (Gray *et al.*, 2005; Jung *et al.*,
151 2008; Li *et al.*, 2019; Xu *et al.*, 2005). Since STAT3 activation is sustained in efferocytic macrophages and considered a hallmark
152 macrophage response to engulfing apoptotic cancer cells it was hypothesized that STAT3 activation is critical in HIF-1 α stabilization by
153 efferocytosis. We investigated this using two well characterized STAT3 inhibitors: Stattic and S3I-201 (Schust *et al.*, 2006; Siddiquee *et*
154 *al.*, 2007). Both inhibitors significantly reduced the activation of STAT3 analyzed after incubation with apoptotic cancer cells for two
155 hours. This treatment also impacted the stabilization of HIF-1 α (Figure 2D-2G and Figure 2–Figure supplement 1). Similarly, these
156 findings were observed in macrophages efferocytosing apoptotic Myc-CaP cells (Figure 2–Figure supplement 2). These findings strongly
157 support the hypothesis that STAT3 activation is a critical signal that mediates the stabilization of HIF-1 α by efferocytosis.

158 To further investigate these findings, a direct interaction between HIF-1 α and p-STAT3 was evaluated in immunoprecipitation assays.
159 Protein lysates collected from macrophages co-cultured with apoptotic prostate cancer RM1 cells were used to perform
160 immunoprecipitation with HIF-1 α -specific antibodies and the pull-down of p-STAT3 was evaluated by Western Blot. The blot showed a
161 p-STAT3 band in the macrophage lysates from efferocytic samples which were immunoprecipitated with HIF-1 α (Figure 2H). The p-
162 STAT3 band was undetected in immunoprecipitated protein samples from non-efferocytic macrophages. These results strongly suggest
163 the interaction between HIF-1 α and p-STAT3 in efferocytic macrophages which support the hypothesis of STAT3 activation as a
164 mechanism mediating the stabilization of HIF-1 α .



165
166
167
168
169
170
171

172 **Figure 2. Macrophage efferocytosis of apoptotic cancer cells promotes HIF-1 α stabilization through STAT3**

173 **activation.**

174 Bone marrow-derived macrophages were isolated from 4 week old C57BL/6J or FVB/NJ mice and co-cultured with apoptotic
175 RM1(a) or Myc-CaP(a) cells for 16-18 hours.

176 **A.** mRNAs isolated from efferocytic and control macrophages were analyzed by quantitative PCR (qPCR) for a set of genes
177 involved in the cellular response to hypoxia (n=9). **B. & C.** Protein lysates from C57BL/6J (n=9) and FVB/NJ (n=6) efferocytic
178 macrophages were analyzed by western blot using HIF-1 α antibody. Protein lysates from C57BL/6J efferocytic and control
179 macrophages (n=3) treated with 5 μ M Stattic and 60 μ M S3I-201 STAT3 inhibitors for 2 hours were analyzed by western blot using
180 **D. & F.** Phospho-STAT3 antibody and **E. & G.** HIF-1 α antibody. **H.** Cell lysates from efferocytic and non-efferocytic macrophages
181 were immunoprecipitated with anti-HIF-1 α antibody and immunoblotted with phospho-STAT3 antibody. Data plotted are mean \pm
182 SEM, *p < 0.05, **p < 0.01, ***p < 0.001, ****p < 0.0001, ns=not significant (Ordinary one-way ANOVA; Tukey's multiple-
183 comparisons test and unpaired t-test). Additional results are shown in Figure 2–Figure supplement 1 and 2.

184 ***Efferocytosis stimulates the expression of pro-inflammatory MIF cytokine in macrophages***

185 Accumulating experimental evidence suggests that efferocytosis of apoptotic cancer cells accelerates tumor progression and metastatic
186 growth by fostering an inflammatory and immunosuppressive microenvironment (Elliott *et al*, 2017; Werfel & Cook, 2018). Single-cell
187 data identified the negative regulation of the immune system process (GO: 0002683; related to the immunosuppressive response) as
188 one of the GO terms upregulated in efferocytic macrophages. Using STRING, a database of known and predicted protein-protein
189 interactions, we identified strong network association between this immune response and the biological process of hypoxia (GO:
190 0071456) (Figure 3A, GO gene list Table 2 and Table 3 in Supplementary data). Although not identified by single cell STAT3 was added
191 because of its key role in the stabilization of HIF-1 α as shown in Figure 2. Central nodes identified in this network are HIF-1 α , Myc and
192 STAT3 and the findings show direct or indirect interactions between hypoxia and the negative immune regulation processes.

193 Furthermore, single cell analysis identified the cytokine macrophage migration inhibitory factor *Mif* as upregulated in efferocytic
194 macrophages (p<10⁻⁶) (Figure 1F, Figure 3B and Figure 3–Figure supplement 1). *Mif* belongs to both GO: 0002683 and GO: 0071456
195 (Gene Ontology, 2021) and mediates both immunosuppression and inflammation and has been associated with increased
196 tumorigenesis and disease progression in different cancer types including prostate cancer (Penticuff *et al*, 2019).

197 MIF changes were investigated in the overall macrophage population co-cultured with apoptotic RM1 prostate cancer cells by RT-qPCR
198 and Western blot. In correlation with single cell results both MIF mRNA (Figure 3C) and protein increased in bone macrophages
199 efferocytosing apoptotic RM1 cells (Figure 3D). Similarly bone marrow macrophages isolated from FVB mice upregulated MIF protein
200 upon efferocytosis of Myc-CaP prostate cancer cells (Figure 3E).

205 These findings indicate MIF is part of the signaling response of macrophages to the engulfing of apoptotic prostate cancer cells and
 206 suggests a network connection with the activation of hypoxia-related molecules by efferocytosis.

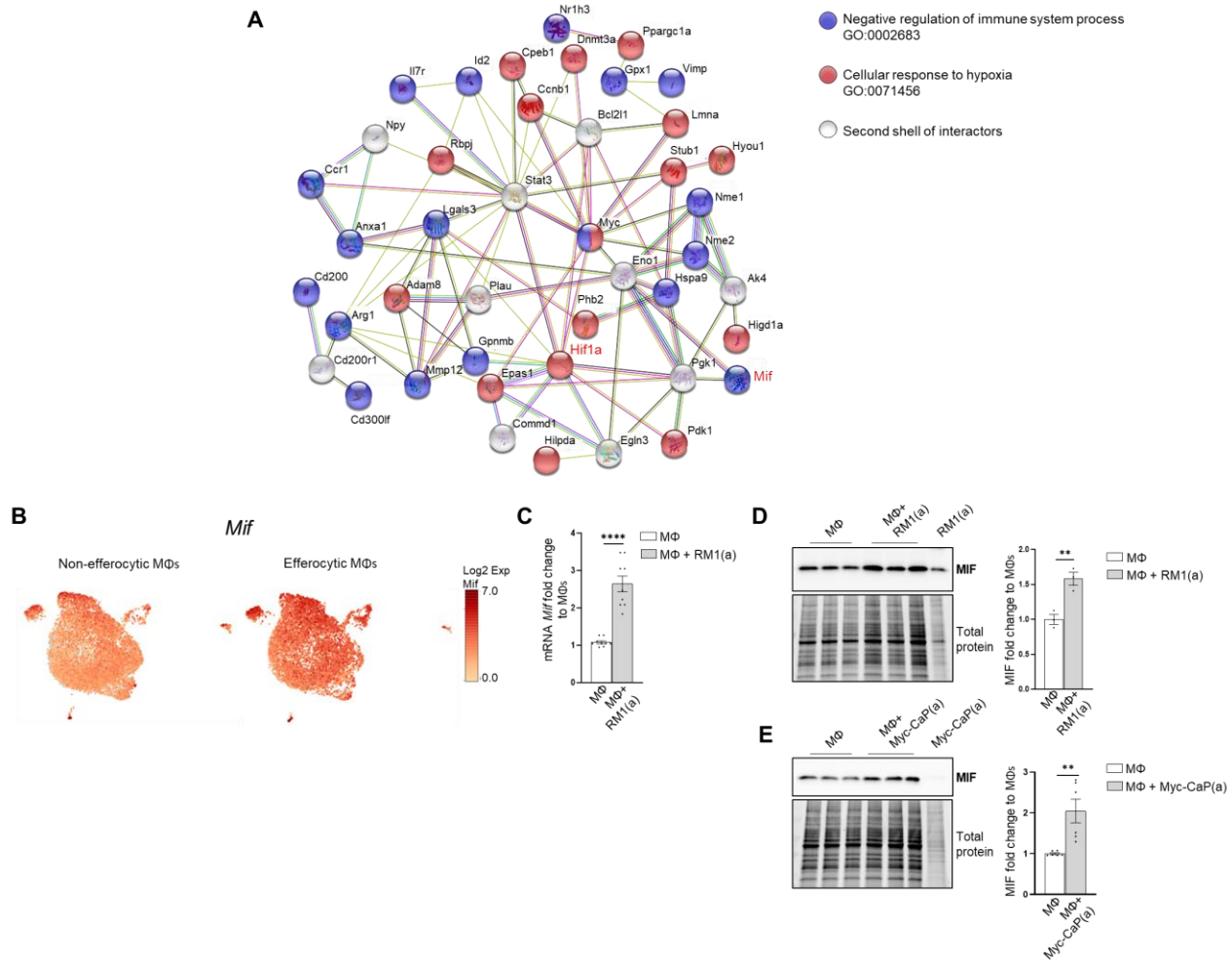


Figure 3. Macrophage efferocytosis induces MIF expression.

A. Protein-protein interaction network between the immune pathway regulation and the hypoxia related pathway. Biological Process GO terms of selected genes upregulated by efferocytosis (GO:0002683, all genes; GO:0071456, 25 out of 33 genes). Bone marrow-derived macrophages were isolated from 4 week old C57BL/6J or FVB/NJ mice and co-cultured with apoptotic RM1(a) or Myc-CaP(a) cells for 16-18 hours. **B.** scRNA-Seq analysis plot shows *Mif* distribution in efferocytic and non-efferocytic clusters of macrophages. **C.** *Mif* mRNA expression in efferocytic macrophages assessed by RT-qPCR (n=9). Western blot analysis of protein lysates from **D.** C57BL/6J macrophages co-cultured with apoptotic RM1 prostate cancer cells (n=3) and **E.** FVB/NJ efferocytic and control macrophages using MIF antibody (n=6). Data plotted are mean ± SEM, **p < 0.01, ****p < 0.0001 (unpaired t-test). Additional results are shown in Figure 3–Figure supplement 1.

HIF-1 α mediates the expression of MIF cytokine in bone efferocytic macrophages

The implication of HIF-1 α in tumor promoting inflammation, immunosuppression and metastasis has been documented in different cancer models in relation to hypoxia (Triner & Shah, 2016). We hypothesized that the stabilization of HIF-1 α in bone macrophages by the clearance of apoptotic cancer cells induces the expression of key pro-inflammatory cytokines. This was investigated by crossing LysM-Cre mice with the HIF-1 α ^{flox/flox} mice to obtain mutated HIF-1 α myeloid lineage mutant mice (*Hif1 α* ^{mut}). These mice create a null allele in the Cre-expressing cells (myeloid) lacking the exon 2 of *Hif1 α* and were used to obtain *Hif1 α* ^{mut} bone macrophages. Relative *Hif1 α* specific mRNAs were quantified with a primer/probe set corresponding to exon 2 of the mRNA. The qPCR analysis showed the upregulation of *Hif1 α* mRNA in the efferocytic macrophages relative to control (Figure 4A). In support of the model a significant decrease in the *Hif1 α* mRNA containing the exon 2 was observed in *Hif1 α* ^{mut} macrophages corresponding to control and efferocytic samples (Figure 4A). In addition, characterization of *Hif1 α* ^{mut} bone marrow derived macrophages by Western blot demonstrated a lower molecular weight in *Hif1 α* ^{mut} which corresponds with the deletion in the DNA binding domain encoded by the exon 2 (Figure 4C) by Cre-induced recombination which renders a non-functional *Hif1 α* ^{mut} protein. However even this mutant protein was stabilized by efferocytosis as shown by quantitative Western blot analyses, which suggests that STAT3-mediated stabilization is independent of HIF-1 α binding to the chromatin (Figure 4C). Of note STAT3 activation remained unaffected in mutant macrophages (Figure 4–Figure supplement 1). Previous studies suggest a link between HIF-1 α and MIF in different cell models, including macrophages (Alonso *et al*, 2019; Baugh *et al*, 2006). We investigated the expression of MIF and other pro-inflammatory factors as potential targets of HIF-1 α . These included critical inflammatory cytokines previously found upregulated in efferocytic macrophages: CXCL1, CXCL5 and IL6 and CXCL4 (also known as platelet factor 4, *Pf4*) (Vaught *et al*, 2015). From the selected cytokines it was found that *Mif* and *Cxcl4* expression was significantly reduced in *Hif1 α* ^{mut} efferocytic macrophages relative to wild type (WT) after normalization to their specific control macrophages (Figure 4B).

Further analysis of MIF protein indicated a significant reduction in MIF protein expression and no upregulation was observed by efferocytosis in the *Hif1 α* ^{mut} macrophages relative to WT (Figure 4D). In contrast upregulation of MIF by efferocytosis was found in WT macrophages as previously shown in (Figure 3D-3E).

To address the specificity of HIF-1 α in the control of MIF regulation, similar experiments were performed with *Epas1*-myeloid lineage-mutant (*Epas1*^{mut}) mice. These mice were obtained by crossing LysM-Cre mice with the *Epas1*^{flox/flox} mice. The mutant mice expressed significantly lower levels of *Epas1* mRNA by RT-qPCR using the primer/probe set corresponding to the deleted exon2 (Figure 4–Figure supplement 2A). In addition, qPCR analysis of pro-inflammatory cytokines indicated a significant decrease in *Cxcl1* in the mutant mice, while no changes in *Mif* and *Cxcl4* (Figure 4–Figure supplement 2B), suggesting *Epas1*- specific regulation of pro-inflammatory cytokines, which is different than the observed for HIF-1 α -mediated regulation in macrophages (Figure 4B). Quantitative protein analysis of mutant macrophages indicated no change by efferocytosis in HIF-1 α stabilization in the *Epas1*^{mut} macrophages relative to WT control (Figure 4–Figure supplement 2C) and no change by efferocytosis in MIF expression when compared mutant versus WT

(Figure 4–Figure supplement 2D) different from the results for efferocytic *Hif1a*^{mut} macrophages (Figure 4D). Furthermore, when analyzed relative to the control macrophages, the efferocytic *Epas1*^{mut} macrophages showed a significant increase in MIF (Figure 4–Figure supplement 2D), while no change was observed in efferocytic *Hif1a*^{mut} macrophages (Figure 4D). These results highlight the specificity in the regulation of MIF expression by HIF-1α relative to EPAS1, a similar hypoxia-inducible transcription factor.

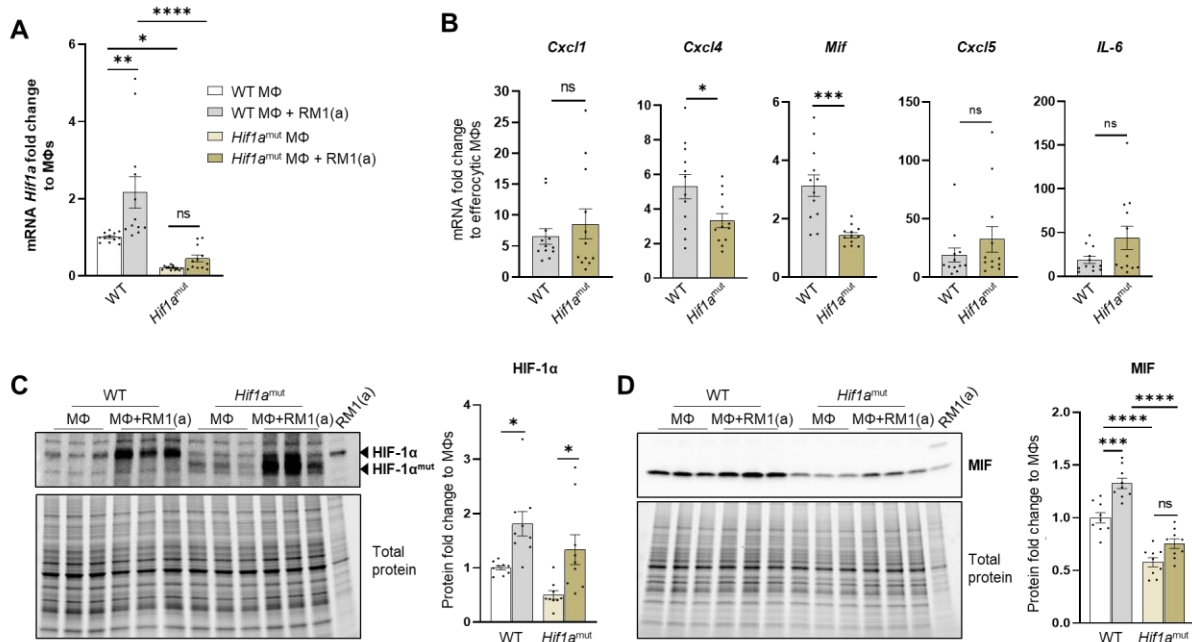
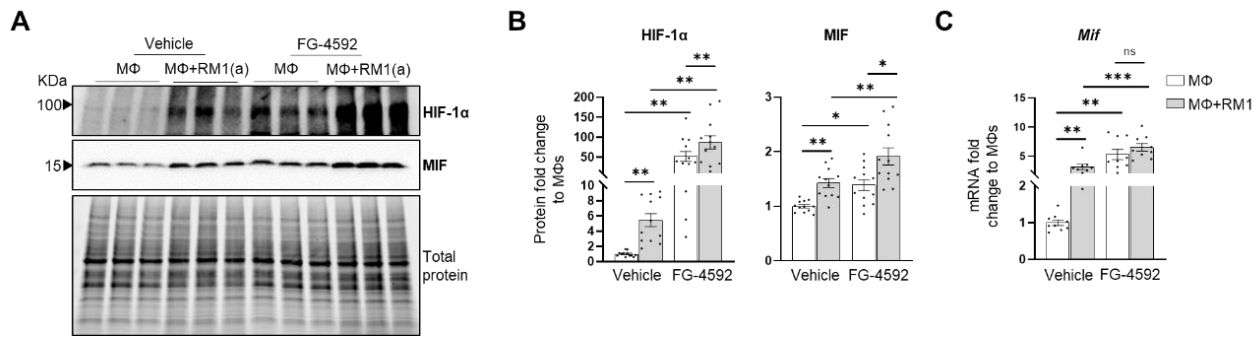


Figure 4. HIF-1α depletion in efferocytic macrophages reduces MIF expression.

A. *Hif1a* mRNA expression levels in *Hif1a*^{fllox/fllox} and *Hif1a*^{mut} macrophages. **B.** mRNA from efferocytic and control macrophages from *Hif1a*^{fllox/fllox} and *Hif1a*^{mut} mice were analyzed by RT-qPCR for the specified inflammatory cytokine genes (n=12). **C. & D.** Protein lysates from efferocytic and control macrophages from *Hif1a*^{fllox/fllox} (WT) and *Hif1a*^{mut} mice were analyzed by Western blot with HIF-1α and MIF antibodies (n=9). Data plotted are mean ± SEM. *p < 0.05, ***p < 0.001, ****p < 0.0001, ns=not significant (Ordinary one-way ANOVA; Tukey's multiple-comparisons test and unpaired t-test). Additional results are shown in Figure 4–Figure supplement 1 and 2.

HIF-1α-mediated MIF regulation was further investigated by using a HIF α-prolyl-hydroxylase inhibitor FG-4592 (also known as Roxadustat) (Hsieh *et al*, 2007). FG-4592 was used in efferocytosis assays, where a strong correlation was observed between the stabilization of HIF-1α and MIF protein expression. FG-4592 alone stabilized HIF-1α which correlated with up-regulation of MIF protein in non-efferocytic macrophages. Intriguingly, when the inhibitor was used in efferocytic macrophages a further increase in HIF-1α and MIF protein was observed (Figure 5A and 5B). RT-qPCR analysis showed a significant increase in *Mif* mRNA induced by FG-4592 relative to control however no further increase was observed in efferocytic macrophages (Figure 5C).

276 Altogether, these findings suggest that HIF-1 α mediates the expression of MIF, where HIF-1 α stabilization by efferocytosis or prolyl-
 277 hydroxylase inhibitor significantly upregulates MIF expression in bone macrophages.



278 **Figure 5. Efferocytic macrophages stabilize HIF-1 α and induce MIF expression.**

279 Bone marrow-derived macrophages were isolated from C57BL/6J mice and co-cultured alone or with apoptotic RM1(a)
 280 cells and treated with FG-4592, HIF prolyl-hydroxylase inhibitor (10 μ M) or vehicle control for 16-18 hours. **A. & B.**
 281 Protein lysates from co-cultures were analyzed by Western blot with HIF-1 α and MIF antibodies (n=12). **C.** mRNAs
 282 were isolated from co-cultures and analyzed by RT-qPCR for *Mif* expression (n=9). Graphs show the fold change
 283 relative to macrophage control for each group. Data plotted are mean \pm SEM; *P<0.05, **P < 0.01, ***p < 0.001,
 284 ns=not significant (Repeated measures one-way ANOVA; Tukey's multiple-comparisons test).
 285

286 ***MIF activates inflammation in bone macrophages***

287 CD74 is a critical receptor for MIF signal transduction in cells; however, CD74 lacks kinase activity and requires a complex formation
 288 with other co-receptors including CD44 and CXCR4 (Bernhagen *et al*, 2007; Leng *et al*, 2003; Shi *et al*, 2006). Results from single-cell
 289 data analyses identified a significant downregulation of CD74 in efferocytic macrophages as compared with non-efferocytic (Figure 6A,
 290 Figure 6–Figure supplement 1), while no significant differences were detected in the co-receptors CD44 or CXCR4. The downregulation
 291 of CD74 was also evident in the overall efferocytic macrophages relative to control by RT-qPCR analyses (Figure 6B).
 292

293 Although these results do not rule out a potential endocrine signaling, they suggest that MIF could induce a potent paracrine signaling
 294 in non-efferocytic macrophages and other cells. To evaluate the MIF-induced signaling in macrophages a purified recombinant MIF
 295 protein expressed in mammalian cells was used. Macrophages were incubated for 2 hours with MIF and signaling activation was
 296 analyzed by Western blot with specific phospho-peptide antibodies. A hallmark MIF transducing signal resulting in the activation
 297 (sustained phosphorylation) of the extracellular signal related kinase ERK1/2 MAPK (Calandra & Roger, 2003; Penticuff *et al*, 2019)
 298 was found highly upregulated in macrophages treated with recombinant MIF protein relative to control (Figure 6C and Figure 6–Figure
 299 supplement 2A). Furthermore, an increase in the critical inflammatory NF- κ B signaling (phospho-p65) was observed in macrophages
 300 treated with MIF (Figure 6C and Figure 6–Figure supplement 2B).
 301

302 This potent inflammation-transduced signaling pathway was further correlated with the increased expression in MIF activated
 303 macrophages of several pro-inflammatory cytokines including: *Ccl5*, *Cxcl5*, *Il6*, *Cxcl1* and *Cxcl4* (Figure 6D and Figure 6–Figure

304 supplement 2B). Similar results were observed in FVB macrophages where MIF activated the expression of these cytokines, except for
 305 *Cxcl4* (Figure 6E). The activation of these cytokines has also been detected in macrophages engulfing prostate cancer cells and
 306 function to accelerate tumor growth in bone as previously demonstrated (Roca & McCauley, 2018). Altogether, these results suggest
 307 that the STAT3-HIF-1 α -MIF is a potent signaling axis induced by efferocytosis of apoptotic cancer cells which may act via paracrine
 308 signaling to perpetuate inflammation.

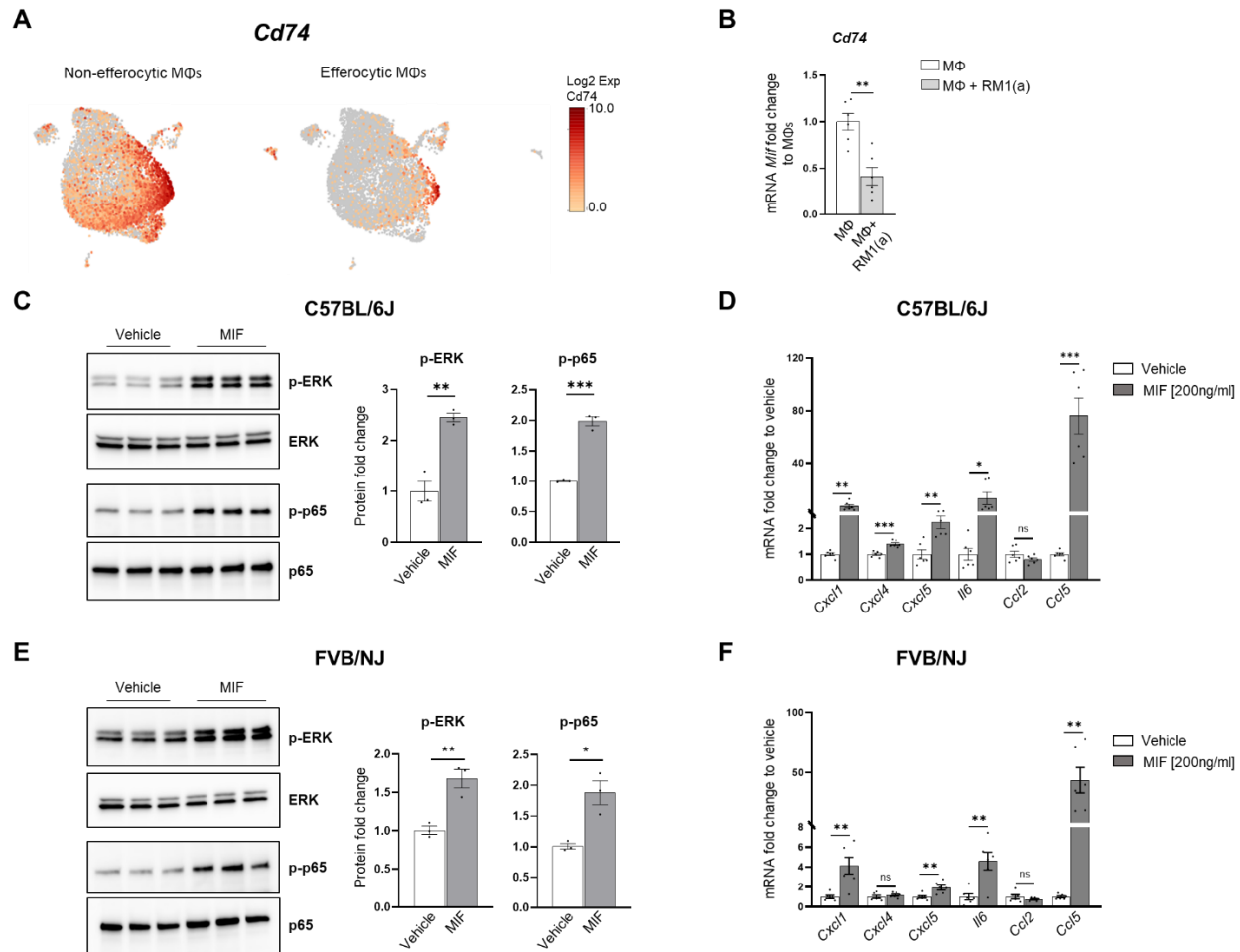


Figure 6. MIF induces a pro-inflammatory response in macrophages

Bone marrow-derived macrophages were isolated from C57BL/6J mice and treated with 200ng/ml of MIF protein or vehicle control during 2 hours for Western blot analysis and 8 hours for mRNA analysis. **A.** scRNA-Seq analysis plot shows *Cd74* distribution in efferocytic and non-efferocytic clusters of macrophages. **B.** *Cd74* mRNA expression in efferocytic macrophages assessed by RT-qPCR (n=6). **C.** Protein lysates from macrophages treated with MIF and vehicle control were analyzed by Western blot with total ERK, p-ERK, total p65 and p-p65 antibodies (n=3). **D.** mRNAs were isolated from co-cultures and analyzed by qPCR for the specified genes (n=6). Data are mean \pm SEM; *p < 0.05, **p < 0.01, ***p < 0.001, ns=not significant (unpaired t-test). Additional results are shown in Figure 6–Figure supplement 1 and 2.

Discussion

Chronic inflammation has a major impact on cancer progression and metastasis in various organs (Coussens & Werb, 2002; Mantovani *et al*, 2008; Trinchieri, 2011). One of the inflammatory mechanisms that promotes tumor growth is the secretion of cytokines and chemokines by cancer and immune cells in the tumor microenvironment (de Visser *et al*, 2006; Quail & Joyce, 2013). Tumor-associated macrophages play a critical role in accelerating tumor progression in different cancer types (Aras & Zaidi, 2017; Duan & Luo, 2021). In bone, apoptotic cancer cell efferocytosis by macrophages generates a unique inflammatory milieu rich in cytokines that promote and support tumor progression (Mendoza-Reinoso *et al.*, 2020; Roca *et al.*, 2018). However, the molecular mechanisms that induce this tumor-promoting inflammatory response in bone marrow macrophages during the efferocytosis of apoptotic prostate cancer cells are still unclear.

Analysis of single-cell transcriptomics of sorted macrophages engulfing apoptotic prostate cancer RM1 cells (efferocytic, F4/80⁺CFSE⁺) versus sorted macrophages alone (non-efferocytic, F4/80⁺) by flow cytometry (Figure 1A) revealed two distinctive clusters of cells, each of them with a unique gene expression profile. Gene ontology term enrichment analysis of the upregulated genes in efferocytic macrophages identified several biological pathways including those directly related to macrophage functions such as response to wounding, innate immune response and regulation of vasculature development (Okabe & Medzhitov, 2016). Although the efferocytosis experiments *in vitro* were conducted under normal oxygen levels, the analysis identified GO-terms related to cell response to hypoxia or decreased oxygen levels in efferocytic macrophages, these terms included genes that are known targets of HIF-1 α , a master transcriptional regulator of cell response to hypoxia (Cui *et al*, 2017). Similarly, hypoxia-independent HIF-1 α expression has been observed in prostate cancer tumors, which correlates with recurrence following surgery or therapy, increased chemoresistance and accelerated metastatic progression, suggesting that alternative mechanisms of post-translational stabilization could lead to its accumulation and transcriptional activity in non-hypoxic environments (Ranasinghe *et al*, 2015; Ranasinghe *et al*, 2014). Here we found that efferocytic bone marrow macrophages promoted HIF-1 α stabilization and induced a strong and sustained phosphorylation of STAT3 under normoxic conditions. Moreover, co-immunoprecipitation experiments performed in this study demonstrated p-STAT3/HIF-1 α interaction in efferocytic macrophages, which correlates with previous studies (Gray *et al.*, 2005; Jung *et al.*, 2008; Jung *et al*, 2005).

Previous studies have associated the expression of HIF-1 α and its target genes with immunosuppressive functions in the tumor microenvironment (Chiavarina *et al*, 2010; Palazon *et al*, 2017). Here we identified a strong protein network association between the genes related to cellular response to hypoxia and negative regulation of the immune response in bone marrow efferocytic macrophages, suggesting that HIF-1 α signaling in efferocytic macrophages may exert immunosuppressive functions in the tumor microenvironment. It has been reported that HIF-1 α promotes the secretion of cytokines and chemokines such as CXC motif chemokine ligand 5 (CXCL5), CXC motif chemokine ligand 12 (CXCL12), chemokine ligand 28 (CCL28), and macrophage migration inhibitory factor

354 (MIF) (Blaisdell *et al.*, 2015; Du *et al.*, 2008; Facciabene *et al.*, 2011; Zhu *et al.*, 2014). One of the genes included in the network
355 analysis was *Mif*. MIF is a pro-inflammatory cytokine expressed by monocytes, macrophages, blood dendritic cells, B cells,
356 neutrophils, eosinophils, mast cells, and basophils; and its expression is involved in both innate and adaptive immune processes, as
357 well as in response to hypoxia. Several studies have shown that MIF mediates inflammatory processes such as sepsis and cancer
358 (Bernhagen *et al.*, 1993; O'Reilly *et al.*, 2016). We demonstrated that MIF mRNA and protein levels were increased in bone marrow
359 macrophages upon efferocytosis of apoptotic cancer cells. MIF is highly expressed in prostate cancer patients and its expression has
360 been associated with higher severity and poor outcome (Meyer-Siegler *et al.*, 2005). Also, it has been reported that HIF-1 α regulates
361 MIF secretion in breast cancer cells to promote tumor proliferation, angiogenesis and metastasis (Larsen *et al.*, 2008). Interestingly, we
362 found that HIF-1 α but not HIF-2 α depletion in bone marrow macrophages reduced the expression of the pro-tumorigenic inflammatory
363 cytokines *Mif* and *Cxcl4* after being exposed to apoptotic prostate cancer cells when compared to wildtype bone marrow macrophages.
364 Furthermore, HIF stabilization by a prolyl-hydroxylase inhibitor further stabilized HIF-1 α and induced MIF mRNA and protein expression
365 in efferocytic bone marrow macrophages. These results suggest that HIF-1 α specifically regulates MIF expression in efferocytic
366 macrophages, which may induce a chronic inflammatory response in the bone tumor microenvironment.

367
368 MIF signals through its main receptor CD74 and its co-receptors CD44, CXCR2, or CXCR4 (Bernhagen *et al.*, 2007; Leng *et al.*, 2003;
369 Shi *et al.*, 2006). MIF/CD74 activity promotes immunosuppressive signaling in macrophages and dendritic cells and inhibition of this
370 signaling reestablishes the antitumor immune response in metastatic melanoma (Figueiredo *et al.*, 2018; Tanese *et al.*, 2015). Moreover,
371 MIF/CD74 signaling also activates the NF- κ B signaling pathway in chronic lymphocytic leukemia (Binsky *et al.*, 2007; Gil-Yarom *et al.*,
372 2017). CD74/CD44 activation by MIF is followed by phosphorylation of the proto-oncogene tyrosine-protein kinase (SRC), extracellular
373 signal-related kinase 1/2 (ERK1/2), phosphoinositide 3-kinase (PI3K), and protein kinase B (AKT) (Gore *et al.*, 2008; Leng *et al.*, 2003;
374 Lue *et al.*, 2007; Shi *et al.*, 2006). These kinases promote the activation of transcription factors such as nuclear factor-kappa B (NF- κ B,
375 p65) which induces the secretion of pro-inflammatory cytokines such as IL-6, IL-8, CCL2 and CCL5 (Abdul-Aziz *et al.*, 2017; Binsky *et al.*
376 *et al.*, 2007; Gregory *et al.*, 2006; Johnson *et al.*, 2018; Xu *et al.*, 2008). Here we found that *Cd74* expression is downregulated in
377 efferocytic bone marrow macrophages, suggesting a paracrine signaling in non-efferocytic macrophages. Recombinant MIF protein
378 treatment of non-efferocytic macrophages activated the ERK1/2 and the NF- κ B (p65) pathways and increased the expression of pro-
379 inflammatory cytokines such as CXCL1, CXCL5, IL-6 and CCL5.

380
381 Altogether, these findings reveal a new regulatory mechanism of HIF-1 α in macrophages during efferocytosis of apoptotic cancer cells
382 where the p-STAT3/HIF-1 α /MIF signaling pathway induces chronic inflammation in the tumor bone microenvironment and promotes
383 the expression of pro-inflammatory cytokines (Figure 7). Since enhanced cell death inevitably occurs during tumor growth and is
384 increased with many cancer therapies our results suggest this pathway becomes highly activated in bone metastatic patients
385 undergoing chemo or radiation therapies and may contribute to increased inflammation and accelerated cancer growth.

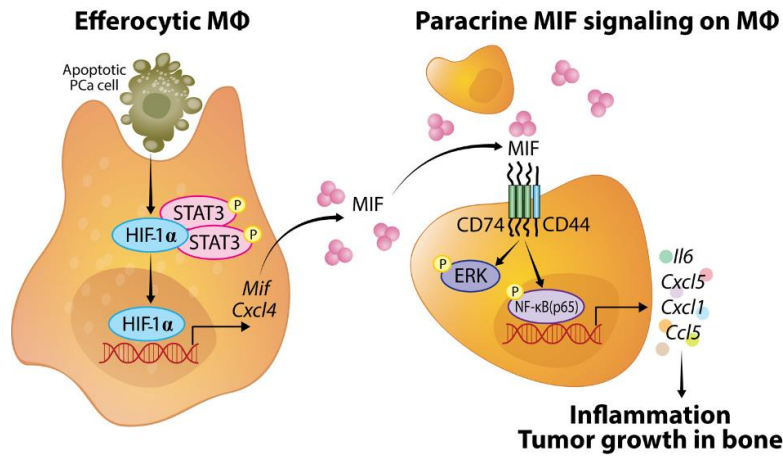


Figure 7. HIF-1α signaling during bone macrophage efferocytosis of apoptotic

cancer cells. Bone macrophage engulfment of apoptotic prostate cancer cells promotes

HIF-1α stability by its interaction with p-STAT3. Once HIF-1α is stabilized it is translocated to

the nucleus to initiate the transcription and secretion of *Mif* and *Cxcl4*. Secreted MIF binds

CD74/CD44 receptor complex of neighboring macrophages and activates ERK1/2 and p65 to

induce the production of pro-inflammatory cytokines in the tumor microenvironment to

support tumor growth in bone.

413 **Material and Methods**

414

415 **Key resources table**

Species/reagent type	Designation	Source of reference	Identifiers	Additional information
Mouse line	C57BL/6J	Jackson Laboratory	C57BL/6J (Stock# 000664)	
Mouse line	FVB/NJ	Jackson Laboratory	FVB/NJ (Stock# 001800)	
Mouse line	<i>Hif1a</i> ^{mut}	Jackson Laboratory	B6.129- <i>Hif1a</i> ^{tm3Rsjc} /J (Stock# 007561)	Contains loxP sites flanking exon 2 of <i>Hif1a</i> (HIF-1α). Exposure to Cre recombinase removes the floxed sequence - creating a null allele.
Mouse line	<i>Epas1</i> ^{mut}	Jackson Laboratory	STOCK <i>Epas1</i> ^{tm1Mcs} /J (Stock# 008407)	Contains loxP sites flanking exon 2 of <i>Epas1</i> (HIF-2α). Exposure to Cre recombinase results in exon 2 deletion.
Mouse line	LysMCre	Jackson Laboratory	B6.129P2- <i>Lyzz</i> ^{tm1(cre)lfo} /J (Stock# 004781)	
Cell line (<i>Mus musculus</i>)	Prostate cancer, fibroblast-like (C57BL/6J)	ATCC	RM1 (ATCC, Cat.# CRL-3310)	Ras+Myc-induced prostate cancer that developed from a urogenital sinus mouse prostate reconstitution.
Cell line (<i>Mus musculus</i>)	Prostate cancer, epithelial-like (FVB/NJ)	ATCC	Myc-CaP (ATCC, Cat.# CRL-3255)	Derived from a genetically engineered mouse prostate cancer removed from an animal that was never exposed to hormone ablation.
Probe	<i>18S</i> (<i>Mus musculus</i>)	ThermoFisher Scientific	TaqMan, assay ID Mm03928990_g1	
Probe	<i>Hif1a</i> (<i>Mus musculus</i>)	ThermoFisher Scientific	TaqMan, assay ID Mm00468869_m1	
Probe	<i>Epas1</i> (<i>Mus musculus</i>)	ThermoFisher Scientific	TaqMan, assay ID Mm01236108_m1	
Probe	<i>Adam8</i> (<i>Mus musculus</i>)	ThermoFisher Scientific	TaqMan, assay ID Mm01163449_g1	
Probe	<i>Hyou1</i> (<i>Mus musculus</i>)	ThermoFisher Scientific	TaqMan, assay ID Mm00491279_m1	
Probe	<i>Pdk1</i> (<i>Mus musculus</i>)	ThermoFisher Scientific	TaqMan, assay ID Mm00554300_m1	
Probe	<i>Stub1</i> (<i>Mus musculus</i>)	ThermoFisher Scientific	TaqMan, assay ID Mm00490634_m1	
Probe	<i>Cpbe1</i> (<i>Mus musculus</i>)	ThermoFisher Scientific	TaqMan, assay ID Mm01314928_m1	
Probe	<i>Pgk1</i> (<i>Mus musculus</i>)	ThermoFisher Scientific	TaqMan, assay ID Mm00435617_m1	
Probe	<i>Myc</i> (<i>Mus musculus</i>)	ThermoFisher Scientific	TaqMan, assay ID Mm00487804_m1	
Probe	<i>Ldha</i> (<i>Mus musculus</i>)	ThermoFisher Scientific	TaqMan, assay ID Mm01612132_g1	
Probe	<i>Mif</i> (<i>Mus musculus</i>)	ThermoFisher Scientific	TaqMan, assay ID Mm01611157_gH	
Probe	<i>Cd74</i> (<i>Mus musculus</i>)	ThermoFisher Scientific	TaqMan, assay ID Mm00658576_m1	
Probe	<i>Cxcl1</i> (<i>Mus musculus</i>)	ThermoFisher Scientific	TaqMan, assay ID Mm04207460_m1	
Probe	<i>Pf4</i> (<i>Mus musculus</i>)	ThermoFisher Scientific	TaqMan, assay ID Mm00451315_g1	
Probe	<i>Cxcl5</i> (<i>Mus musculus</i>)	ThermoFisher Scientific	TaqMan, assay ID Mm00436451_g1	
Probe	<i>Il6</i> (<i>Mus musculus</i>)	ThermoFisher Scientific	TaqMan, assay ID Mm00446190_m1	
Probe	<i>Ccl2</i> (<i>Mus musculus</i>)	ThermoFisher Scientific	TaqMan, assay ID Mm00441242_m1	
Probe	<i>Ccl5</i> (<i>Mus musculus</i>)	ThermoFisher Scientific	TaqMan, assay ID Mm01302427_m1	
Primers	B6.129- <i>Hif1a</i> ^{tm3Rsjc} /J (genotyping)			Forward: 5'-TGCATGTGTATGGGTGTTTTG-3' Reverse: 5'-GAAACTGTCTGTAACCTTCATTTCC-3'
Primers	STOCK <i>Epas1</i> ^{tm1Mcs} /J (genotyping)			Forward: 5'-GAGAGCAGCTTCTCCTGGAA-3' Reverse: 5'-TGTAGGCAAGGAAACCAAGG-3'
Primers	B6.129P2- <i>Lyzz</i> ^{tm1(cre)lfo} /J (genotyping)			Mutant: 5'-CCCAGAAATGCCAGATTACG-3' Common: 5'-CTTGGGCTGCCAGAAATTTCTC-3' Wildtype: 5'-TTACAGTCGGCCAGGCTGAC-3'
Antibody	Anti HIF-1α (D1S7W) XP, Rabbit monoclonal	Cell Signaling Technology	Cat.# 36169	WB (1:2000); IP (1:50)
Antibody	Anti MIF, Rabbit polyclonal	Cell Signaling Technology	Cat.# 88186	WB (1:3000)
Antibody	Anti-phospho Stat3 (Tyr705) (D3A7) XP®, Rabbit monoclonal	Cell Signaling Technology	Cat.# 9145	WB (1:3000)
Antibody	Anti Stat3 (124H6), Mouse monoclonal	Cell Signaling Technology	Cat.# 9139	WB (1:2000)
Antibody	Anti-phospho-Stat3 (Tyr705) (3E2), Mouse monoclonal	Cell Signaling Technology	Cat.# 9138	WB (1:2000)
Antibody	Anti p44/42 MAPK (Erk1/2) (137F5), Rabbit monoclonal	Cell Signaling Technology	Cat.# 4695	WB (1:3000)
Antibody	Anti-phospho p44/42 MAPK (Erk1/2) (Thr202/Tyr204) (D13.14.4E) XP®, Rabbit monoclonal	Cell Signaling Technology	Cat.# 4370	WB (1:3000)
Antibody	Anti NFκB p65 (D14E12) XP®, Rabbit monoclonal	Cell Signaling Technology	Cat.# 8242	WB (1:3000)
Antibody	Anti-phospho NF-κB p65 (Ser536) (93H1), Rabbit monoclonal	Cell Signaling Technology	Cat.# 3033	WB (1:3000)
Antibody	APC Anti-F4/80 antibody [Cl:A3-1] (Allophycocyanin)	Abcam	Cat.# ab105080	FC (1:100)
Antibody	APC Rat IgG2b, kappa monoclonal [KLH/G2b-1-2] - Isotype control (Allophycocyanin)	Abcam	Cat.# ab154434	FC (1:100)

416

417

418 **Animals and cell lines**

419 All animal experiments were performed with approval from the University of Michigan Institutional Animal Care and Use Committee.

420 Immunocompetent C57BL/6J, FVB/NJ, B6.129P2-*Lyzz*^{tm1(cre)lfo}/J (LysMCre), B6.129-*Hif1a*^{tm3Rsjc}/J (HIF-1α^{lox}) (Ryan *et al*, 2000) and

421 *Epas1^{tm1Mcs/J}* (HIF-2 α^{floX}) (Gruber *et al*, 2007) mice were purchased from the Jackson Laboratory (Bar Harbor, ME, USA). The HIF-1 α^{floX}
422 and HIF-2 α^{floX} mice were crossed consecutively with LysMCre mice to achieve the Hif1 $\alpha^{\text{floX/floX-LysMCre}^{+/-}}$ (*Hif1 α^{mut}*) and *Epas1^{flox/flox}*-
423 LysMCre $^{+/-}$ (*Epas1^{mut}*) mice that exhibit HIF-1 α and HIF-2 α inactivation in myeloid cells including macrophages. HIF-1 $\alpha^{\text{floX/floX}}$ and HIF-
424 2 $\alpha^{\text{floX/floX}}$ mice were used as experimental controls.

425 RM1 is a (Ras+Myc)-induced prostate cancer cell line developed in C57BL/6J mice and was a gift from Timothy C. Thompson (Baylor
426 College of Medicine, Houston, TX, USA) (Baley *et al*, 1995; Thompson *et al*, 1989). Myc-CaP prostate cancer cell line is derived from a
427 prostate carcinoma from a Hi-Myc FVB/NJ mice and was donated by Russell Taichman and Frank Cackowski (University of Michigan,
428 Ann Arbor, MI, USA) (Watson *et al*, 2005). Both cell lines were cultured on RPMI 1640 media containing 10% fetal bovine serum (FBS)
429 and grown at 37°C with ambient O₂ and 5% CO₂.

431 ***Murine efferocytosis in vitro model***

432 Bone marrow-derived macrophages (MΦs) were isolated from 4–6 week old male C57BL/6J, FVB/NJ, *Hif1 α^{mut}* , *Epas1^{mut}*, HIF-1 α^{floX} and
433 HIF-2 α^{floX} mice by flushing the femur and tibia with minimum essential medium eagle - alpha modification (αMEM) supplemented with
434 L-glutamine, antibiotic-antimycotic 1× and 10% fetal bovine serum (FBS). Macrophages were cultured in αMEM (L-glutamine,
435 antibiotic-antimycotic 1×, 10% FBS) in the presence of macrophage colony stimulating factor (M-CSF) (30 ng/mL, #315-02, Peprotech,
436 Rocky Hill, NJ, USA). After three days in culture, macrophages were plated independently at 2 × 10⁶ cells/well in αMEM (L-glutamine,
437 antibiotic-antimycotic 1×, 0.25% FBS) for co-culture experiments. RM1 and Myc-CaP cells were exposed to UV light for 30 min to
438 induce apoptosis. Apoptotic (a) cells (>90% trypan blue incorporation) were co-cultured with macrophages at a 1:1 ratio in αMEM (L-
439 glutamine, 0.25% FBS) for 16–18 h. Macrophages from mutant mice were compared with those from respective littermate controls.

440
441 Prolyl hydroxylase inhibition in efferocytic and non-efferocytic macrophages was performed using 10μM Roxadustat (FG-4592) (Cayman
442 Chemical, 15294) for 16–18 hours. STAT3 inhibition in efferocytic and non-efferocytic macrophages was performed using 5μM Stattic
443 (Cayman Chemical, 14590) or 60μM S3I-201 (Millipore Sigma, SML0330) for 10 minutes, then media was replaced and incubated for an
444 additional 2 hours. Macrophages alone were treated with 200ng/ml of recombinant MIF protein (SinoBiological, 50066-M08H) during 2
445 hours for Western blot analysis and 8 hours for RNA expression analysis.

447 ***Single-cell library preparation and RNA sequencing***

448 A modified murine efferocytosis *in vitro* model was used. Apoptotic RM1 cells were labeled with CellTrace™ CFSE (ThermoFisher
449 Scientific, C34554), and then co-cultured with macrophages for 16–18 h. Efferocytic and non-efferocytic macrophages were collected
450 and incubated in fluorescence-activated cell sorter (FACS) staining buffer (phosphate buffered saline-1X, 0.2% bovine serum albumin).
451 F4/80 antibody and isotype control were added and incubated for 1 h at 4 °C. F4/80⁺ only (non-efferocytic macrophages) and
452 F4/80⁺CFSE⁺ (efferocytic macrophages) were sorted using a BD FACSAria™ III (BD biosciences, San Jose, CA, USA). Antibody
453 information is available in Key resources table.

454

455

The single cell scRNA-seq libraries were prepared at the University of Michigan Advanced Genomics Core using the 10X Genomics Chromium Next GEM Single Cell 3' Kit v3.1 (part number 1000268) following the manufacturer's protocol. Cell suspensions were diluted to target a recovery of 10,000 cells per sample. The libraries were run on an Agilent TapeStation 4200 (part number G2991BA) for library quality control before sequencing. Libraries were sequenced at a depth of 50,000 reads/cell on a NovaSeq6000 with the following run configuration: Read 1 - 150 cycles; i7 index read - 8 cycles; Read 2 - 150 cycles.

460

461

Single-cell RNA-sequencing analysis and visualization

462

463

464

465

466

467

468

469

470

471

The sequenced data was processed using the 10X Genomics CellRanger software suite v3.0.0. Briefly, fastq files from each of the samples were mapped to the Mouse genome mm10 and genes were counted using CellRanger software and the STAR aligner (Dobin *et al*, 2013). The barcode-gene matrices were further analyzed using the Seurat R package (v3.1) (Butler *et al*, 2018). Following standard practices to remove low-quality cells, cells that expressed less than 200 genes or less than 1,000 transcripts, or had greater than 10% mitochondrial genes were filtered from the datasets (Supplementary Table 1). For genes, only the top 5,000 variable genes were included for downstream analysis. Samples were then normalized and integrated according to the Seurat suggested pipeline. To reduce the dimensionality of the samples, we first performed a principal component analysis (PCA). The number of principle components for further downstream applications were 20, and UMAP was employed for final dimensionality reduction and visualization of the data.

472

Differential Expression and Gene Ontology Analysis

473

474

475

476

477

Differential expression analysis was conducted using the DESingle R package (Miao *et al*, 2018). Genes with a false discovery rate adjusted p-value < 0.05 were considered differentially expressed. For pathway analysis, we used PANTHER analysis (Mi *et al*, 2013; Thomas *et al*, 2003) with the gene ontology database (Ashburner *et al*, 2000; Gene Ontology, 2021). Only genes differentially expressed and up-regulated in the efferocytic macrophages in both experiments were included in the GSEA analysis.

478

Western blot analysis and co-immunoprecipitation assay

479

480

481

482

483

484

485

486

Whole cell lysate was extracted in Cell Lysis Buffer 1X (Cell signaling, 9803) containing 1X protease and phosphatase inhibitor cocktail (ThermoFisher Scientific, 78440). Estimation of protein concentration was done using Bradford assay (BioRad, 5000006). Samples were diluted using 1X Laemmli Sample Buffer (4X stock, BioRad, 1610747) with 10% β -Mercaptoethanol (Millipore Sigma, M3148). Protein lysates were separated using 4-20% Mini-PROTEAN® TGX Stain-Free™ gels (BioRad, 4568096) and transferred to PVDF membrane using the Trans-Blot Turbo RTA kit (BioRad, 1704272). The membrane was blocked with 5% milk in 1X TBS- 0.1% Tween for 1 hour at room temperature, then incubated with primary antibodies in 5% BSA during overnight at 4°C. Secondary antibody was diluted in 5% milk in 1X TBS- 0.1% Tween. For co-immunoprecipitation assays macrophage and apoptotic prostate cancer cell co-cultures were lysed on ice with 1% Triton X-100 in 1X PBS with 1X protease and phosphatase inhibitor cocktail. Whole cell lysates were

487 immunoprecipitated using HIF-1 α antibody and protein A-magnetic beads (Cell Signaling Technology, 73778) during overnight
488 incubation at 4°C. Binding and washing were performed in the same lysis buffer followed by immunoblotting with appropriate
489 antibodies. Blots were developed using SuperSignal™ West Femto Maximum Sensitivity Substrate (ThermoFisher Scientific, 34095).
490 Protein gels used for protein normalization and blots were imaged using the ChemiDoc™ MP Imaging System (BioRad, 12003154).
491 Antibody information is available in Methods - Key resources table.

493 ***RT-qPCR***

494 Cells were harvested using RNeasy Mini Kit (Qiagen, 74106) RNA was eluted with nuclease-free water. The RNA was quantified using a
495 NanoDrop 2000 (Thermo Scientific) and cDNA was synthesized 1 μ g of RNA per 20 μ l reaction mixture using High-Capacity cDNA
496 Reverse Transcription Kit (ThermoFisher Scientific, 4368814). RT-qPCR was performed using TaqMan® probes and Gene Expression
497 qPCR Assays TaqMan Gene Express (ThermoFisher Scientific, 4369016) with 40 cycles on an ABI PRISM 7700 (Applied Biosystems,
498 Foster City, CA, USA). The analysis was performed using 2- $\Delta\Delta$ CT method (Schmittgen & Livak, 2008). TaqMan® probes information is
499 available in Key resources table.

501 ***Statistics***

502 Statistical analyses were performed using GraphPad Prism 9 (GraphPad Software, version 9.1.0, San Diego, CA, USA) using ordinary
503 and repeated measures one-way analysis of variance (ANOVA) with Tukey's multiple-comparisons, and unpaired t-tests analyses with
504 significance of $p < 0.05$.

506 ***Data availability***

507
508 Raw sequencing data for both experiments: Experiment 1 (GSM5466517/roca4, non-efferocytic and GSM5466518/roca5, efferocytic).
509 Experiment 2 (GSM5466519/roca6, non-efferocytic and GSM5466520/roca7, efferocytic) are deposited in the NCBI Sequence Read
510 Archive (SRA) and can be accessed from the NCBI Gene Expression Omnibus (GEO, Series Accession: GSE180638).

512 ***Funding***

513
514 This work was supported by NIH award P01-CA093900 to L.K.M and E.T.K. DoD award EIRA-W81XWH-21-1-0122 log#PC200058 to
515 V.M.-R.

517 ***Acknowledgements***

518
519 The authors would like to thank the University of Michigan Advanced Genomics Core for the single-cell processing and sequencing of

the samples, and the Rogel Cancer Center Single Cell Analysis Core for further analysis of the single-cell data included in this study.

Conflicts of Interest

The authors declare no conflict of interest.

References

- Abdul-Aziz AM, Shafat MS, Mehta TK, Di Palma F, Lawes MJ, Rushworth SA, Bowles KM (2017) MIF-Induced Stromal PKCbeta/IL8 Is Essential in Human Acute Myeloid Leukemia. *Cancer Res* 77: 303-311. <https://doi.org/10.1158/0008-5472.CAN-16-1095>
- Alonso D, Serrano E, Bermejo FJ, Corral RS (2019) HIF-1alpha-regulated MIF activation and Nox2-dependent ROS generation promote Leishmania amazonensis killing by macrophages under hypoxia. *Cell Immunol* 335: 15-21. <https://doi.org/10.1016/j.cellimm.2018.10.007>
- Aras S, Zaidi MR (2017) TAMEless traitors: macrophages in cancer progression and metastasis. *Br J Cancer* 117: 1583-1591. <https://doi.org/10.1038/bjc.2017.356>
- Ashburner M, Ball CA, Blake JA, Botstein D, Butler H, Cherry JM, Davis AP, Dolinski K, Dwight SS, Eppig JT *et al* (2000) Gene ontology: tool for the unification of biology. The Gene Ontology Consortium. *Nat Genet* 25: 25-29. <https://doi.org/10.1038/75556>
- Bach JP, Rinn B, Meyer B, Dodel R, Bacher M (2008) Role of MIF in inflammation and tumorigenesis. *Oncology* 75: 127-133. <https://doi.org/10.1159/000155223>
- Baley PA, Yoshida K, Qian W, Sehgal I, Thompson TC (1995) Progression to androgen insensitivity in a novel in vitro mouse model for prostate cancer. *J Steroid Biochem Mol Biol* 52: 403-413. [https://doi.org/10.1016/0960-0760\(95\)00001-g](https://doi.org/10.1016/0960-0760(95)00001-g)
- Baugh JA, Gantier M, Li L, Byrne A, Buckley A, Donnelly SC (2006) Dual regulation of macrophage migration inhibitory factor (MIF) expression in hypoxia by CREB and HIF-1. *Biochem Biophys Res Commun* 347: 895-903. <https://doi.org/10.1016/j.bbrc.2006.06.148>
- Becht E, McInnes L, Healy J, Dutertre CA, Kwok IWH, Ng LG, Ginhoux F, Newell EW (2018) Dimensionality reduction for visualizing single-cell data using UMAP. *Nat Biotechnol* <https://doi.org/10.1038/nbt.4314>
- Bernhagen J, Calandra T, Mitchell RA, Martin SB, Tracey KJ, Voelter W, Manogue KR, Cerami A, Bucala R (1993) MIF is a pituitary-derived cytokine that potentiates lethal endotoxaemia. *Nature* 365: 756-759. <https://doi.org/10.1038/365756a0>
- Bernhagen J, Krohn R, Lue H, Gregory JL, Zerneck A, Koenen RR, Dewor M, Georgiev I, Schober A, Leng L *et al* (2007) MIF is a noncognate ligand of CXC chemokine receptors in inflammatory and atherogenic cell recruitment. *Nat Med* 13: 587-596. <https://doi.org/10.1038/nm1567>
- Binsky I, Haran M, Starlets D, Gore Y, Lantner F, Harpaz N, Leng L, Goldenberg DM, Shvidel L, Berrebi A *et al* (2007) IL-8 secreted in a macrophage migration-inhibitory factor- and CD74-dependent manner regulates B cell chronic lymphocytic leukemia survival. *Proc Natl Acad Sci U S A* 104: 13408-13413. <https://doi.org/10.1073/pnas.0701553104>
- Blaisdell A, Crequer A, Columbus D, Daikoku T, Mittal K, Dey SK, Erlebacher A (2015) Neutrophils Oppose Uterine Epithelial Carcinogenesis

553 via Debridement of Hypoxic Tumor Cells. *Cancer Cell* 28: 785-799. <https://doi.org/10.1016/j.ccell.2015.11.005>

554 Blouin CC, Page EL, Soucy GM, Richard DE (2004) Hypoxic gene activation by lipopolysaccharide in macrophages: implication of hypoxia-
555 inducible factor 1alpha. *Blood* 103: 1124-1130. <https://doi.org/10.1182/blood-2003-07-2427>

556 Bucala R, Donnelly SC (2007) Macrophage migration inhibitory factor: a probable link between inflammation and cancer. *Immunity* 26:
557 281-285. <https://doi.org/10.1016/j.immuni.2007.03.005>

558 Butler A, Hoffman P, Smibert P, Papalexi E, Satija R (2018) Integrating single-cell transcriptomic data across different conditions,
559 technologies, and species. *Nat Biotechnol* 36: 411-420. <https://doi.org/10.1038/nbt.4096>

560 Calandra T, Roger T (2003) Macrophage migration inhibitory factor: a regulator of innate immunity. *Nat Rev Immunol* 3: 791-800.
561 <https://doi.org/10.1038/nri1200>

562 Chiavarina B, Whitaker-Menezes D, Migneco G, Martinez-Outschoorn UE, Pavlides S, Howell A, Tanowitz HB, Casimiro MC, Wang C, Pestell
563 RG *et al* (2010) HIF1-alpha functions as a tumor promoter in cancer associated fibroblasts, and as a tumor suppressor in breast cancer
564 cells: Autophagy drives compartment-specific oncogenesis. *Cell Cycle* 9: 3534-3551. <https://doi.org/10.4161/cc.9.17.12908>

565 Coussens LM, Werb Z (2002) Inflammation and cancer. *Nature* 420: 860-867. <https://doi.org/10.1038/nature01322>

566 Cramer T, Yamanishi Y, Clausen BE, Forster I, Pawlinski R, Mackman N, Haase VH, Jaenisch R, Corr M, Nizet V *et al* (2003) HIF-1alpha
567 is essential for myeloid cell-mediated inflammation. *Cell* 112: 645-657. [https://doi.org/10.1016/s0092-8674\(03\)00154-5](https://doi.org/10.1016/s0092-8674(03)00154-5)

568 Cui XG, Han ZT, He SH, Wu XD, Chen TR, Shao CH, Chen DL, Su N, Chen YM, Wang T *et al* (2017) HIF1/2alpha mediates hypoxia-
569 induced LDHA expression in human pancreatic cancer cells. *Oncotarget* 8: 24840-24852. <https://doi.org/10.18632/oncotarget.15266>

570 de Visser KE, Eichten A, Coussens LM (2006) Paradoxical roles of the immune system during cancer development. *Nat Rev Cancer* 6: 24-
571 37. <https://doi.org/10.1038/nrc1782>

572 Dobin A, Davis CA, Schlesinger F, Drenkow J, Zaleski C, Jha S, Batut P, Chaisson M, Gingeras TR (2013) STAR: ultrafast universal RNA-
573 seq aligner. *Bioinformatics* 29: 15-21. <https://doi.org/10.1093/bioinformatics/bts635>

574 Du R, Lu KV, Petritsch C, Liu P, Ganss R, Passegue E, Song H, Vandenberg S, Johnson RS, Werb Z *et al* (2008) HIF1alpha induces the
575 recruitment of bone marrow-derived vascular modulatory cells to regulate tumor angiogenesis and invasion. *Cancer Cell* 13: 206-220.
576 <https://doi.org/10.1016/j.ccr.2008.01.034>

577 Duan Z, Luo Y (2021) Targeting macrophages in cancer immunotherapy. *Signal Transduct Target Ther* 6: 127.
578 <https://doi.org/10.1038/s41392-021-00506-6>

579 Dudzinski SO, Cameron BD, Wang J, Rathmell JC, Giorgio TD, Kirschner AN (2019) Combination immunotherapy and radiotherapy causes
580 an abscopal treatment response in a mouse model of castration resistant prostate cancer. *J Immunother Cancer* 7: 218.
581 <https://doi.org/10.1186/s40425-019-0704-z>

582 Elliott MR, Koster KM, Murphy PS (2017) Efferocytosis Signaling in the Regulation of Macrophage Inflammatory Responses. *J Immunol*
583 198: 1387-1394. <https://doi.org/10.4049/jimmunol.1601520>

584 Ellwood-Yen K, Graeber TG, Wongvipat J, Iruela-Arispe ML, Zhang J, Matusik R, Thomas GV, Sawyers CL (2003) Myc-driven murine
585 prostate cancer shares molecular features with human prostate tumors. *Cancer Cell* 4: 223-238. <https://doi.org/10.1016/s1535->

- 586 [6108\(03\)00197-1](https://doi.org/10.1101/2021.09.02.458687)
- 587 Engel C, Brugmann G, Lambing S, Muhlenbeck LH, Marx S, Hagen C, Horvath D, Goldeck M, Ludwig J, Herzner AM *et al* (2017) RIG-I
588 Resists Hypoxia-Induced Immunosuppression and Dedifferentiation. *Cancer Immunol Res* 5: 455-467. [https://doi.org/10.1158/2326-](https://doi.org/10.1158/2326-6066.CIR-16-0129-T)
589 [6066.CIR-16-0129-T](https://doi.org/10.1158/2326-6066.CIR-16-0129-T)
- 590 Facciabene A, Peng X, Hagemann IS, Balint K, Barchetti A, Wang LP, Gimotty PA, Gilks CB, Lal P, Zhang L *et al* (2011) Tumour hypoxia
591 promotes tolerance and angiogenesis via CCL28 and T(reg) cells. *Nature* 475: 226-230. <https://doi.org/10.1038/nature10169>
- 592 Figueiredo CR, Azevedo RA, Mousdell S, Resende-Lara PT, Ireland L, Santos A, Girola N, Cunha R, Schmid MC, Polonelli L *et al* (2018)
593 Blockade of MIF-CD74 Signalling on Macrophages and Dendritic Cells Restores the Antitumour Immune Response Against Metastatic
594 Melanoma. *Front Immunol* 9: 1132. <https://doi.org/10.3389/fimmu.2018.01132>
- 595 Gene Ontology C (2021) The Gene Ontology resource: enriching a GOLD mine. *Nucleic Acids Res* 49: D325-D334.
596 <https://doi.org/10.1093/nar/gkaa1113>
- 597 Gil-Yarom N, Radomir L, Sever L, Kramer MP, Lewinsky H, Bornstein C, Blecher-Gonen R, Barnett-Itzhaki Z, Mirkin V, Friedlander G *et al*
598 (2017) CD74 is a novel transcription regulator. *Proc Natl Acad Sci U S A* 114: 562-567. <https://doi.org/10.1073/pnas.1612195114>
- 599 Gore Y, Starlets D, Maharshak N, Becker-Herman S, Kaneyuki U, Leng L, Bucala R, Shachar I (2008) Macrophage migration inhibitory
600 factor induces B cell survival by activation of a CD74-CD44 receptor complex. *J Biol Chem* 283: 2784-2792.
601 <https://doi.org/10.1074/jbc.M703265200>
- 602 Graham DK, DeRyckere D, Davies KD, Earp HS (2014) The TAM family: phosphatidylserine sensing receptor tyrosine kinases gone awry
603 in cancer. *Nat Rev Cancer* 14: 769-785. <https://doi.org/10.1038/nrc3847>
- 604 Gray MJ, Zhang J, Ellis LM, Semenza GL, Evans DB, Watowich SS, Gallick GE (2005) HIF-1alpha, STAT3, CBP/p300 and Ref-1/APE are
605 components of a transcriptional complex that regulates Src-dependent hypoxia-induced expression of VEGF in pancreatic and prostate
606 carcinomas. *Oncogene* 24: 3110-3120. <https://doi.org/10.1038/sj.onc.1208513>
- 607 Gregory JL, Morand EF, McKeown SJ, Ralph JA, Hall P, Yang YH, McColl SR, Hickey MJ (2006) Macrophage migration inhibitory factor
608 induces macrophage recruitment via CC chemokine ligand 2. *J Immunol* 177: 8072-8079. <https://doi.org/10.4049/jimmunol.177.11.8072>
- 609 Gruber M, Hu CJ, Johnson RS, Brown EJ, Keith B, Simon MC (2007) Acute postnatal ablation of Hif-2alpha results in anemia. *Proc Natl*
610 *Acad Sci U S A* 104: 2301-2306. <https://doi.org/10.1073/pnas.0608382104>
- 611 Hartmann H, Eltzschig HK, Wurz H, Hantke K, Rakin A, Yazdi AS, Matteoli G, Bohn E, Autenrieth IB, Karhausen J *et al* (2008) Hypoxia-
612 independent activation of HIF-1 by enterobacteriaceae and their siderophores. *Gastroenterology* 134: 756-767.
613 <https://doi.org/10.1053/j.gastro.2007.12.008>
- 614 Hatfield S, Veszeleiova K, Steingold J, Sethuraman J, Sitkovsky M (2019) Mechanistic Justifications of Systemic Therapeutic Oxygenation
615 of Tumors to Weaken the Hypoxia Inducible Factor 1alpha-Mediated Immunosuppression. *Adv Exp Med Biol* 1136: 113-121.
616 https://doi.org/10.1007/978-3-030-12734-3_8
- 617 Hayashi Y, Yokota A, Harada H, Huang G (2019) Hypoxia/pseudohypoxia-mediated activation of hypoxia-inducible factor-1alpha in cancer.
618 *Cancer Sci* 110: 1510-1517. <https://doi.org/10.1111/cas.13990>

619 Hsieh MM, Linde NS, Wynter A, Metzger M, Wong C, Langsetmo I, Lin A, Smith R, Rodgers GP, Donahue RE *et al* (2007) HIF prolyl
620 hydroxylase inhibition results in endogenous erythropoietin induction, erythrocytosis, and modest fetal hemoglobin expression in rhesus
621 macaques. *Blood* 110: 2140-2147. <https://doi.org/10.1182/blood-2007-02-073254>

622 Hu CJ, Wang LY, Chodosh LA, Keith B, Simon MC (2003) Differential roles of hypoxia-inducible factor 1alpha (HIF-1alpha) and HIF-2alpha
623 in hypoxic gene regulation. *Mol Cell Biol* 23: 9361-9374. <https://doi.org/10.1128/MCB.23.24.9361-9374.2003>

624 Imtiyaz HZ, Williams EP, Hickey MM, Patel SA, Durham AC, Yuan LJ, Hammond R, Gimotty PA, Keith B, Simon MC (2010) Hypoxia-
625 inducible factor 2alpha regulates macrophage function in mouse models of acute and tumor inflammation. *J Clin Invest* 120: 2699-2714.
626 <https://doi.org/10.1172/JCI39506>

627 Ivan M, Kondo K, Yang H, Kim W, Valiando J, Ohh M, Salic A, Asara JM, Lane WS, Kaelin WG, Jr. (2001) HIFalpha targeted for VHL-
628 mediated destruction by proline hydroxylation: implications for O2 sensing. *Science* 292: 464-468.
629 <https://doi.org/10.1126/science.1059817>

630 Jaakkola P, Mole DR, Tian YM, Wilson MI, Gielbert J, Gaskell SJ, von Kriegsheim A, Hebestreit HF, Mukherji M, Schofield CJ *et al* (2001)
631 Targeting of HIF-alpha to the von Hippel-Lindau ubiquitylation complex by O2-regulated prolyl hydroxylation. *Science* 292: 468-472.
632 <https://doi.org/10.1126/science.1059796>

633 Johnson DE, O'Keefe RA, Grandis JR (2018) Targeting the IL-6/JAK/STAT3 signalling axis in cancer. *Nat Rev Clin Oncol* 15: 234-248.
634 <https://doi.org/10.1038/nrclinonc.2018.8>

635 Jung JE, Kim HS, Lee CS, Shin YJ, Kim YN, Kang GH, Kim TY, Juhn YS, Kim SJ, Park JW *et al* (2008) STAT3 inhibits the degradation of
636 HIF-1alpha by pVHL-mediated ubiquitination. *Exp Mol Med* 40: 479-485. <https://doi.org/10.3858/emm.2008.40.5.479>

637 Jung JE, Lee HG, Cho IH, Chung DH, Yoon SH, Yang YM, Lee JW, Choi S, Park JW, Ye SK *et al* (2005) STAT3 is a potential modulator of
638 HIF-1-mediated VEGF expression in human renal carcinoma cells. *FASEB J* 19: 1296-1298. <https://doi.org/10.1096/fj.04-3099fje>

639 Kaelin WG, Jr., Ratcliffe PJ (2008) Oxygen sensing by metazoans: the central role of the HIF hydroxylase pathway. *Mol Cell* 30: 393-402.
640 <https://doi.org/10.1016/j.molcel.2008.04.009>

641 Koh TJ, DiPietro LA (2011) Inflammation and wound healing: the role of the macrophage. *Expert Rev Mol Med* 13: e23.
642 <https://doi.org/10.1017/S1462399411001943>

643 Lantz C, Radmanesh B, Liu E, Thorp EB, Lin J (2020) Single-cell RNA sequencing uncovers heterogenous transcriptional signatures in
644 macrophages during efferocytosis. *Sci Rep* 10: 14333. <https://doi.org/10.1038/s41598-020-70353-y>

645 Larsen M, Tazzyman S, Lund EL, Junker N, Lewis CE, Kristjansen PE, Murdoch C (2008) Hypoxia-induced secretion of macrophage
646 migration-inhibitory factor from MCF-7 breast cancer cells is regulated in a hypoxia-inducible factor-independent manner. *Cancer Lett*
647 265: 239-249. <https://doi.org/10.1016/j.canlet.2008.02.012>

648 Lecoultre M, Dutoit V, Walker PR (2020) Phagocytic function of tumor-associated macrophages as a key determinant of tumor progression
649 control: a review. *J Immunother Cancer* 8 <https://doi.org/10.1136/jitc-2020-001408>

650 Leng L, Metz CN, Fang Y, Xu J, Donnelly S, Baugh J, Delohery T, Chen Y, Mitchell RA, Bucala R (2003) MIF signal transduction initiated
651 by binding to CD74. *J Exp Med* 197: 1467-1476. <https://doi.org/10.1084/jem.20030286>

- 652 Li J, Shen J, Wang Z, Xu H, Wang Q, Chai S, Fu P, Huang T, Anas O, Zhao H *et al* (2019) ELTD1 facilitates glioma proliferation, migration
653 and invasion by activating JAK/STAT3/HIF-1 α signaling axis. *Sci Rep* 9: 13904. <https://doi.org/10.1038/s41598-019-50375-x>
- 654 Lippitz BE (2013) Cytokine patterns in patients with cancer: a systematic review. *Lancet Oncol* 14: e218-228.
655 [https://doi.org/10.1016/S1470-2045\(12\)70582-X](https://doi.org/10.1016/S1470-2045(12)70582-X)
- 656 Lue H, Thiele M, Franz J, Dahl E, Speckgens S, Leng L, Fingerle-Rowson G, Bucala R, Luscher B, Bernhagen J (2007) Macrophage
657 migration inhibitory factor (MIF) promotes cell survival by activation of the Akt pathway and role for CSN5/JAB1 in the control of autocrine
658 MIF activity. *Oncogene* 26: 5046-5059. <https://doi.org/10.1038/sj.onc.1210318>
- 659 Mantovani A, Allavena P, Sica A, Balkwill F (2008) Cancer-related inflammation. *Nature* 454: 436-444.
660 <https://doi.org/10.1038/nature07205>
- 661 Mawhinney L, Armstrong ME, C OR, Bucala R, Leng L, Fingerle-Rowson G, Fayne D, Keane MP, Tynan A, Maher L *et al* (2015) Macrophage
662 migration inhibitory factor (MIF) enzymatic activity and lung cancer. *Mol Med* 20: 729-735. <https://doi.org/10.2119/molmed.2014.00136>
- 663 Mendoza-Reinoso V, Baek DY, Kurutz A, Rubin JR, Koh AJ, McCauley LK, Roca H (2020) Unique Pro-Inflammatory Response of
664 Macrophages during Apoptotic Cancer Cell Clearance. *Cells* 9 <https://doi.org/10.3390/cells9020429>
- 665 Meyer-Siegler KL, Iczkowski KA, Vera PL (2005) Further evidence for increased macrophage migration inhibitory factor expression in
666 prostate cancer. *BMC Cancer* 5: 73. <https://doi.org/10.1186/1471-2407-5-73>
- 667 Mi H, Muruganujan A, Thomas PD (2013) PANTHER in 2013: modeling the evolution of gene function, and other gene attributes, in the
668 context of phylogenetic trees. *Nucleic Acids Res* 41: D377-386. <https://doi.org/10.1093/nar/gks1118>
- 669 Miao Z, Deng K, Wang X, Zhang X (2018) DEsingle for detecting three types of differential expression in single-cell RNA-seq data.
670 *Bioinformatics* 34: 3223-3224. <https://doi.org/10.1093/bioinformatics/bty332>
- 671 Minutti CM, Knipper JA, Allen JE, Zaiss DM (2017) Tissue-specific contribution of macrophages to wound healing. *Semin Cell Dev Biol* 61:
672 3-11. <https://doi.org/10.1016/j.semcdb.2016.08.006>
- 673 Niu G, Briggs J, Deng J, Ma Y, Lee H, Kortylewski M, Kujawski M, Kay H, Cress WD, Jove R *et al* (2008) Signal transducer and activator
674 of transcription 3 is required for hypoxia-inducible factor-1 α RNA expression in both tumor cells and tumor-associated myeloid cells.
675 *Mol Cancer Res* 6: 1099-1105. <https://doi.org/10.1158/1541-7786.MCR-07-2177>
- 676 O'Reilly C, Doroudian M, Mawhinney L, Donnelly SC (2016) Targeting MIF in Cancer: Therapeutic Strategies, Current Developments, and
677 Future Opportunities. *Med Res Rev* 36: 440-460. <https://doi.org/10.1002/med.21385>
- 678 Okabe Y, Medzhitov R (2016) Tissue biology perspective on macrophages. *Nat Immunol* 17: 9-17. <https://doi.org/10.1038/ni.3320>
- 679 Palazon A, Goldrath AW, Nizet V, Johnson RS (2014) HIF transcription factors, inflammation, and immunity. *Immunity* 41: 518-528.
680 <https://doi.org/10.1016/j.immuni.2014.09.008>
- 681 Palazon A, Tyrakis PA, Macias D, Velica P, Rundqvist H, Fitzpatrick S, Vojnovic N, Phan AT, Loman N, Hedenfalk I *et al* (2017) An HIF-
682 1 α /VEGF-A Axis in Cytotoxic T Cells Regulates Tumor Progression. *Cancer Cell* 32: 669-683 e665.
683 <https://doi.org/10.1016/j.ccell.2017.10.003>
- 684 Penticuff JC, Woolbright BL, Sielecki TM, Weir SJ, Taylor JA, 3rd (2019) MIF family proteins in genitourinary cancer: tumorigenic roles

685 and therapeutic potential. *Nat Rev Urol* 16: 318-328. <https://doi.org/10.1038/s41585-019-0171-9>

686 Peyssonnaud C, Datta V, Cramer T, Doedens A, Theodorakis EA, Gallo RL, Hurtado-Ziola N, Nizet V, Johnson RS (2005) HIF-1alpha
687 expression regulates the bactericidal capacity of phagocytes. *J Clin Invest* 115: 1806-1815. <https://doi.org/10.1172/JCI23865>

688 Pouyssegur J, Dayan F, Mazure NM (2006) Hypoxia signalling in cancer and approaches to enforce tumour regression. *Nature* 441: 437-
689 443. <https://doi.org/10.1038/nature04871>

690 Quail DF, Joyce JA (2013) Microenvironmental regulation of tumor progression and metastasis. *Nat Med* 19: 1423-1437.
691 <https://doi.org/10.1038/nm.3394>

692 Ranasinghe WK, Baldwin GS, Bolton D, Shulkes A, Ischia J, Patel O (2015) HIF1alpha expression under normoxia in prostate cancer--
693 which pathways to target? *J Urol* 193: 763-770. <https://doi.org/10.1016/j.juro.2014.10.085>

694 Ranasinghe WK, Baldwin GS, Shulkes A, Bolton D, Patel O (2014) Normoxic regulation of HIF-1alpha in prostate cancer. *Nat Rev Urol* 11:
695 419. <https://doi.org/10.1038/nrurol.2013.110-c2>

696 Roca H, Jones JD, Purica MC, Weidner S, Koh AJ, Kuo R, Wilkinson JE, Wang Y, Daignault-Newton S, Pienta KJ *et al* (2018) Apoptosis-
697 induced CXCL5 accelerates inflammation and growth of prostate tumor metastases in bone. *J Clin Invest* 128: 248-266.
698 <https://doi.org/10.1172/JCI92466>

699 Roca H, McCauley LK (2018) Efferocytosis and prostate cancer skeletal metastasis: implications for intervention. *Oncoscience* 5: 174-
700 176. <https://doi.org/10.18632/oncoscience.440>

701 Ryan HE, Poloni M, McNulty W, Elson D, Gassmann M, Arbeit JM, Johnson RS (2000) Hypoxia-inducible factor-1alpha is a positive factor
702 in solid tumor growth. *Cancer Res* 60: 4010-4015.

703 Schmittgen TD, Livak KJ (2008) Analyzing real-time PCR data by the comparative C(T) method. *Nat Protoc* 3: 1101-1108.
704 <https://doi.org/10.1038/nprot.2008.73>

705 Schust J, Sperl B, Hollis A, Mayer TU, Berg T (2006) Stattic: a small-molecule inhibitor of STAT3 activation and dimerization. *Chem Biol*
706 13: 1235-1242. <https://doi.org/10.1016/j.chembiol.2006.09.018>

707 Semenza GL (2011) Oxygen sensing, homeostasis, and disease. *N Engl J Med* 365: 537-547. <https://doi.org/10.1056/NEJMra1011165>

708 Shi X, Leng L, Wang T, Wang W, Du X, Li J, McDonald C, Chen Z, Murphy JW, Lolis E *et al* (2006) CD44 is the signaling component of
709 the macrophage migration inhibitory factor-CD74 receptor complex. *Immunity* 25: 595-606.
710 <https://doi.org/10.1016/j.immuni.2006.08.020>

711 Siddiquee K, Zhang S, Guida WC, Blaskovich MA, Greedy B, Lawrence HR, Yip ML, Jove R, McLaughlin MM, Lawrence NJ *et al* (2007)
712 Selective chemical probe inhibitor of Stat3, identified through structure-based virtual screening, induces antitumor activity. *Proc Natl Acad*
713 *Sci U S A* 104: 7391-7396. <https://doi.org/10.1073/pnas.0609757104>

714 Soki FN, Koh AJ, Jones JD, Kim YW, Dai J, Keller ET, Pienta KJ, Atabai K, Roca H, McCauley LK (2014) Polarization of prostate cancer-
715 associated macrophages is induced by milk fat globule-EGF factor 8 (MFG-E8)-mediated efferocytosis. *J Biol Chem* 289: 24560-24572.
716 <https://doi.org/10.1074/jbc.M114.571620>

717 Stanford JC, Young C, Hicks D, Owens P, Williams A, Vaught DB, Morrison MM, Lim J, Williams M, Brantley-Sieders DM *et al* (2014)

- 718 Efferocytosis produces a prometastatic landscape during postpartum mammary gland involution. *J Clin Invest* 124: 4737-4752.
719 <https://doi.org/10.1172/JCI76375>
- 720 Talks KL, Turley H, Gatter KC, Maxwell PH, Pugh CW, Ratcliffe PJ, Harris AL (2000) The expression and distribution of the hypoxia-
721 inducible factors HIF-1alpha and HIF-2alpha in normal human tissues, cancers, and tumor-associated macrophages. *Am J Pathol* 157:
722 411-421. [https://doi.org/10.1016/s0002-9440\(10\)64554-3](https://doi.org/10.1016/s0002-9440(10)64554-3)
- 723 Tanese K, Hashimoto Y, Berkova Z, Wang Y, Samaniego F, Lee JE, Ekmekcioglu S, Grimm EA (2015) Cell Surface CD74-MIF Interactions
724 Drive Melanoma Survival in Response to Interferon-gamma. *J Invest Dermatol* 135: 2901. <https://doi.org/10.1038/jid.2015.259>
- 725 Tarnowski M, Grymula K, Liu R, Tarnowska J, Drukala J, Ratajczak J, Mitchell RA, Ratajczak MZ, Kucia M (2010) Macrophage migration
726 inhibitory factor is secreted by rhabdomyosarcoma cells, modulates tumor metastasis by binding to CXCR4 and CXCR7 receptors and
727 inhibits recruitment of cancer-associated fibroblasts. *Mol Cancer Res* 8: 1328-1343. <https://doi.org/10.1158/1541-7786.MCR-10-0288>
- 728 Thomas PD, Campbell MJ, Kejariwal A, Mi H, Karlak B, Daverman R, Diemer K, Muruganujan A, Narechania A (2003) PANTHER: a library
729 of protein families and subfamilies indexed by function. *Genome Res* 13: 2129-2141. <https://doi.org/10.1101/gr.772403>
- 730 Thompson TC, Southgate J, Kitchener G, Land H (1989) Multistage carcinogenesis induced by ras and myc oncogenes in a reconstituted
731 organ. *Cell* 56: 917-930. [https://doi.org/10.1016/0092-8674\(89\)90625-9](https://doi.org/10.1016/0092-8674(89)90625-9)
- 732 Tomiyasu M, Yoshino I, Suemitsu R, Okamoto T, Sugimachi K (2002) Quantification of macrophage migration inhibitory factor mRNA
733 expression in non-small cell lung cancer tissues and its clinical significance. *Clin Cancer Res* 8: 3755-3760.
- 734 Trinchieri G (2011) Inflammation in cancer: a therapeutic target? *Oncology (Williston Park)* 25: 418-420.
- 735 Triner D, Shah YM (2016) Hypoxia-inducible factors: a central link between inflammation and cancer. *J Clin Invest* 126: 3689-3698.
736 <https://doi.org/10.1172/JCI84430>
- 737 Vaught DB, Stanford JC, Cook RS (2015) Efferocytosis creates a tumor microenvironment supportive of tumor survival and metastasis.
738 *Cancer Cell Microenviron* 2 <https://doi.org/10.14800/ccm.666>
- 739 Watson PA, Ellwood-Yen K, King JC, Wongvipat J, Lebeau MM, Sawyers CL (2005) Context-dependent hormone-refractory progression
740 revealed through characterization of a novel murine prostate cancer cell line. *Cancer Res* 65: 11565-11571. <https://doi.org/10.1158/0008-5472.CAN-05-3441>
- 741 [5472.CAN-05-3441](https://doi.org/10.1158/0008-5472.CAN-05-3441)
- 742 Werfel TA, Cook RS (2018) Efferocytosis in the tumor microenvironment. *Semin Immunopathol* 40: 545-554.
743 <https://doi.org/10.1007/s00281-018-0698-5>
- 744 Wilson JM, Coletta PL, Cuthbert RJ, Scott N, MacLennan K, Hawcroft G, Leng L, Lubetsky JB, Jin KK, Lolis E *et al* (2005) Macrophage
745 migration inhibitory factor promotes intestinal tumorigenesis. *Gastroenterology* 129: 1485-1503.
746 <https://doi.org/10.1053/j.gastro.2005.07.061>
- 747 Winner M, Koong AC, Rendon BE, Zundel W, Mitchell RA (2007) Amplification of tumor hypoxic responses by macrophage migration
748 inhibitory factor-dependent hypoxia-inducible factor stabilization. *Cancer Res* 67: 186-193. <https://doi.org/10.1158/0008-5472.CAN-06-3292>
- 749 [3292](https://doi.org/10.1158/0008-5472.CAN-06-3292)
- 750 Xu Q, Briggs J, Park S, Niu G, Kortylewski M, Zhang S, Gritsko T, Turkson J, Kay H, Semenza GL *et al* (2005) Targeting Stat3 blocks both

751 HIF-1 and VEGF expression induced by multiple oncogenic growth signaling pathways. *Oncogene* 24: 5552-5560.
752 <https://doi.org/10.1038/sj.onc.1208719>

753 Xu X, Wang B, Ye C, Yao C, Lin Y, Huang X, Zhang Y, Wang S (2008) Overexpression of macrophage migration inhibitory factor induces
754 angiogenesis in human breast cancer. *Cancer Lett* 261: 147-157. <https://doi.org/10.1016/j.canlet.2007.11.028>

755 Yao K, Shida S, Selvakumaran M, Zimmerman R, Simon E, Schick J, Haas NB, Balke M, Ross H, Johnson SW *et al* (2005) Macrophage
756 migration inhibitory factor is a determinant of hypoxia-induced apoptosis in colon cancer cell lines. *Clin Cancer Res* 11: 7264-7272.
757 <https://doi.org/10.1158/1078-0432.CCR-05-0135>

758 Zhu G, Tang Y, Geng N, Zheng M, Jiang J, Li L, Li K, Lei Z, Chen W, Fan Y *et al* (2014) HIF-alpha/MIF and NF-kappaB/IL-6 axes contribute
759 to the recruitment of CD11b+Gr-1+ myeloid cells in hypoxic microenvironment of HNSCC. *Neoplasia* 16: 168-179.
760 <https://doi.org/10.1593/neo.132034>

761
762
763
764
765
766
767
768
769
770
771
772
773
774
775
776
777
778
779
780
781
782
783

784 **Supplementary data**

785

786 **Table 1.** Features of the data included in the single-cell RNA sequencing analysis.

Sample	# of cells	# of unique genes per cell	# of transcripts per cell	Ave. mitochondrial %
Non-efferocytic MΦ (1)	7,813	3,029	12,837	3.39
Efferocytic MΦ (1)	6,262	3,726	19,768	3.18
Non-efferocytic MΦ (2)	10,612	2,909	11,326	2.89
Efferocytic MΦ (2)	7,984	3,800	17,984	3.27

787

788

789 **Table 2.** Selected GO terms (Figure 1E) enriched in efferocytic bone marrow macrophages.

GO term biological process	# of Genes in Term	# of GO term genes in upload list	Expected	Fold enrichment	Raw P-value	FDR value
Regulation of innate immune response (GO:0045088)	287	16	6.08	2.63	6.38E-04	3.89E-02
Cellular response to hypoxia (GO:0071456)	82	13	1.74	7.49	8.25E-08	2.90E-05
Cellular response to decreased oxygen levels (GO:0036294)	86	13	1.82	7.14	1.36E-07	4.20E-05
Cellular response to oxygen levels (GO:0071453)	101	14	2.14	6.55	1.18E-07	3.80E-05
Translational initiation (GO:0006413)	54	13	1.14	11.37	1.02E-09	9.44E-07
Regulation of protein stability (GO:0031647)	278	17	5.89	2.89	1.58E-04	1.44E-02
Positive regulation of vasculature development (GO:1904018)	200	17	4.23	4.02	3.13E-06	5.38E-04
Regulation of response to wounding (GO:1903034)	187	14	3.96	3.54	8.34E-05	8.73E-03
Response to oxidative stress (GO:0006979)	338	23	7.16	3.21	2.22E-06	4.27E-04
Negative regulation of immune system process (GO:0002683)	469	23	9.93	2.32	3.04E-04	2.35E-02

790

791

792

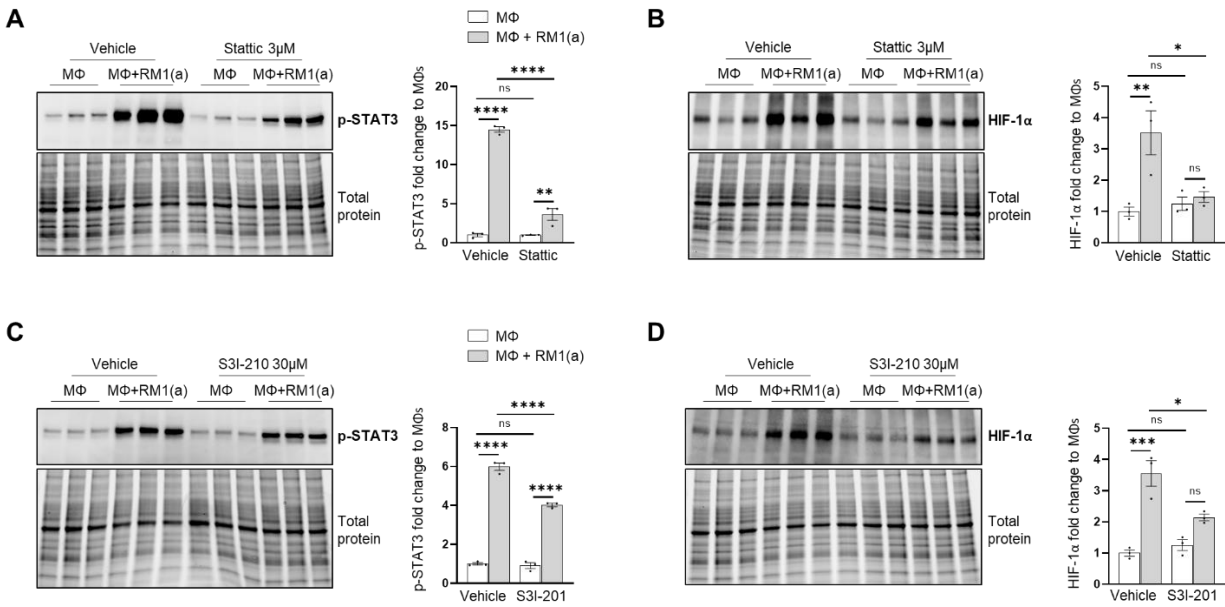
793 **Table 3.** List of upregulated genes from GO terms shown in Figure 1E and Table 2.

Regulation of innate immune response (GO:0045088)	Cellular response to hypoxia (GO:0071456)	Cellular response to decreased oxygen levels (GO:0036294)	Cellular response to oxygen levels (GO:0071453)	Translational initiation (GO:0006413)	Regulation of protein stability (GO:0031647)	Positive regulation of vasculature development (GO:1904018)	Regulation of response to wounding (GO:1903034)	Response to oxidative stress (GO:0006979)	Negative regulation of immune system process (GO:0002683)
<i>Cadm1</i>	<i>Egln3</i>	<i>Egln3</i>	<i>Egln3</i>	<i>Eif4a1</i>	<i>Hypk</i>	<i>Kdr</i>	<i>Plau</i>	<i>Ndufa12</i>	<i>Cb1b</i>
<i>Ccr1</i>	<i>Hyou1</i>	<i>Hyou1</i>	<i>Hyou1</i>	<i>Denr</i>	<i>Rnf128</i>	<i>Mydgf</i>	<i>Cd109</i>	<i>Prdx1</i>	<i>Nme2</i>
<i>Ube2k</i>	<i>Ak4</i>	<i>Ak4</i>	<i>Ak4</i>	<i>Eif3b</i>	<i>Stub1</i>	<i>Ilgax</i>	<i>Anxa1</i>	<i>Sod2</i>	<i>Anxa1</i>
<i>Adam8</i>	<i>Ppargc1a</i>	<i>Ppargc1a</i>	<i>Ppargc1a</i>	<i>Eif4e2</i>	<i>Commnd1</i>	<i>Fgf2</i>	<i>Cd9</i>	<i>Gsr</i>	<i>Selenos</i>
<i>Hsp90aa1</i>	<i>Eno1</i>	<i>Eno1</i>	<i>Eno1</i>	<i>Eif4ebp1</i>	<i>Hip1</i>	<i>Hyal1</i>	<i>Fgf2</i>	<i>Srxn1</i>	<i>Ccr1</i>
<i>Rala</i>	<i>Pgk1</i>	<i>Pgk1</i>	<i>Pgk1</i>	<i>Eif5a</i>	<i>Hsp90aa1</i>	<i>Ago2</i>	<i>Cd36</i>	<i>Ppargc1a</i>	<i>Gpnmb</i>
<i>Arg1</i>	<i>Ndnf</i>	<i>Ndnf</i>	<i>Ndnf</i>	<i>Eif6</i>	<i>Phb2</i>	<i>Sphk1</i>	<i>Anxa2</i>	<i>Nme2</i>	<i>Cd200r1</i>
<i>Mmp12</i>	<i>Epas1</i>	<i>Epas1</i>	<i>Epas1</i>	<i>Eif1a</i>	<i>Rnf149</i>	<i>Il1a</i>	<i>Rtn4r</i>	<i>Apex1</i>	<i>Mif</i>
<i>Psm14</i>	<i>Rbpj</i>	<i>Rbpj</i>	<i>Rbpj</i>	<i>Eif4g1</i>	<i>Plpp3</i>	<i>Pkm</i>	<i>Flna</i>	<i>Anxa1</i>	<i>Il1r</i>
<i>Psm1</i>	<i>Stub1</i>	<i>Stub1</i>	<i>Stub1</i>	<i>Eif4e</i>	<i>Cct8</i>	<i>Lgals3</i>	<i>Pdgfa</i>	<i>Epas1</i>	<i>Nr1h3</i>
<i>Psm7</i>	<i>Commnd1</i>	<i>Commnd1</i>	<i>Commnd1</i>	<i>Eif1ax</i>	<i>Hspd1</i>	<i>Hspa4</i>	<i>Spp1</i>	<i>Selenos</i>	<i>Hspa9</i>
<i>Psm12</i>	<i>Adam8</i>	<i>Adam8</i>	<i>Adam8</i>	<i>Ago2</i>	<i>B4galt5</i>	<i>Angpt2</i>	<i>Mif</i>	<i>Gpx1</i>	<i>Rala</i>
<i>Psmc5</i>	<i>Pdk1</i>	<i>Pdk1</i>	<i>Pdk1</i>	<i>Eif2s1</i>	<i>Lmna</i>	<i>Nrp1</i>	<i>F7</i>	<i>Atf4</i>	<i>Gpx1</i>
<i>Psmb5</i>	<i>Lmna</i>	<i>Lmna</i>	<i>Lmna</i>	<i>Atf4</i>	<i>Ptges3</i>	<i>Hmga2</i>	<i>Plpp3</i>	<i>Cd36</i>	<i>Arg1</i>
<i>Psmb6</i>	<i>Eif4eb1</i>	<i>Eif4eb1</i>	<i>Eif4eb1</i>	<i>Atf3</i>	<i>Hyal1</i>	<i>Flna</i>	<i>Plaur</i>	<i>Hyal1</i>	<i>Cd200</i>
<i>Nr1h3</i>	<i>Myc</i>	<i>Myc</i>	<i>Myc</i>	<i>Cct3</i>	<i>Cct3</i>	<i>Cct3</i>	<i>Rwdd1</i>	<i>Rwdd1</i>	<i>Mmp12</i>
<i>Psm12</i>	<i>Plau</i>	<i>Plau</i>	<i>Plau</i>	<i>Ank2</i>	<i>Ank2</i>	<i>Ank2</i>	<i>Arl6ip5</i>	<i>Arl6ip5</i>	<i>Myc</i>
	<i>Cpeb1</i>	<i>Cpeb1</i>	<i>Cpeb1</i>	<i>Ppargc1a</i>	<i>Ppargc1a</i>	<i>Ppargc1a</i>	<i>Eif2s1</i>	<i>Eif2s1</i>	<i>Nme1</i>
	<i>Mif</i>	<i>Mif</i>	<i>Mif</i>				<i>Pdk1</i>	<i>Pdk1</i>	<i>Cd300lf</i>
	<i>Dnmt3a</i>	<i>Dnmt3a</i>	<i>Dnmt3a</i>				<i>Ndufs8</i>	<i>Ndufs8</i>	<i>Lgals3</i>
	<i>Hilpda</i>	<i>Hilpda</i>	<i>Hilpda</i>				<i>Sphk1</i>	<i>Sphk1</i>	<i>Npy</i>
	<i>Phb2</i>	<i>Phb2</i>	<i>Phb2</i>				<i>Psmb5</i>	<i>Psmb5</i>	<i>Id2</i>
	<i>Higd1a</i>	<i>Higd1a</i>	<i>Higd1a</i>				<i>Pon2</i>	<i>Pon2</i>	<i>Ig1c1</i>
	<i>Ccnb1</i>	<i>Ccnb1</i>	<i>Ccnb1</i>				<i>Cygb</i>	<i>Cygb</i>	
	<i>Bcl2l1</i>	<i>Bcl2l1</i>	<i>Bcl2l1</i>				<i>Pcna</i>	<i>Pcna</i>	
	<i>Psm14</i>	<i>Psm14</i>	<i>Psm14</i>				<i>Hspd1</i>	<i>Hspd1</i>	
	<i>Psm7</i>	<i>Psm7</i>	<i>Psm7</i>				<i>Mif</i>	<i>Mif</i>	
	<i>Psm12</i>	<i>Psm12</i>	<i>Psm12</i>				<i>Il1a</i>	<i>Il1a</i>	
	<i>Psmc5</i>	<i>Psmc5</i>	<i>Psmc5</i>				<i>Hk3</i>	<i>Hk3</i>	
	<i>Psmb5</i>	<i>Psmb5</i>	<i>Psmb5</i>				<i>Ldha</i>	<i>Ldha</i>	
	<i>Psm6</i>	<i>Psm6</i>	<i>Psm6</i>				<i>Bcl2l1</i>	<i>Bcl2l1</i>	
	<i>Psm2</i>	<i>Psm2</i>	<i>Psm2</i>				<i>Arg1</i>	<i>Arg1</i>	
	<i>Psm1</i>	<i>Psm1</i>	<i>Psm1</i>				<i>Cyca</i>	<i>Cyca</i>	
	<i>Atf4</i>	<i>Atf4</i>	<i>Atf4</i>				<i>G6pdx</i>	<i>G6pdx</i>	
		<i>Atp6v1a</i>	<i>Atp6v1a</i>				<i>Atf1</i>	<i>Atf1</i>	
							<i>Scara3</i>	<i>Scara3</i>	
							<i>Por</i>	<i>Por</i>	

794

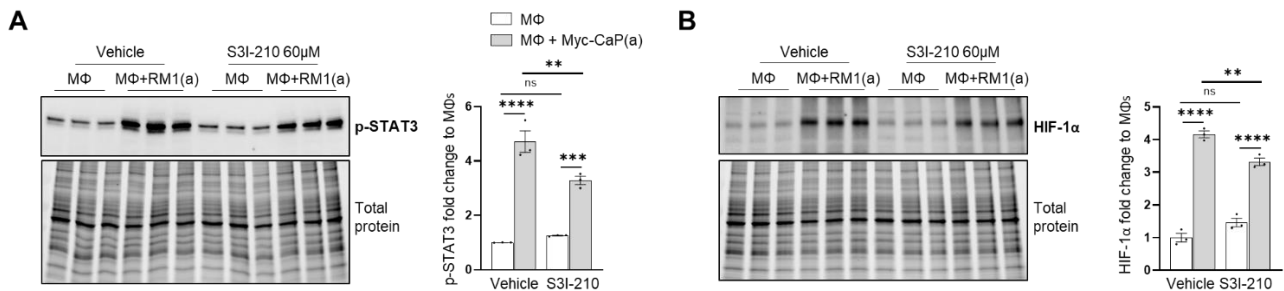
795
796
797

Figure 2–Figure supplement 1. STAT3 inhibition (Stattic and S3I-201) in C57BL/6J in bone marrow macrophages efferocytosing apoptotic prostate cancer RM1 cells (n=3 per group).



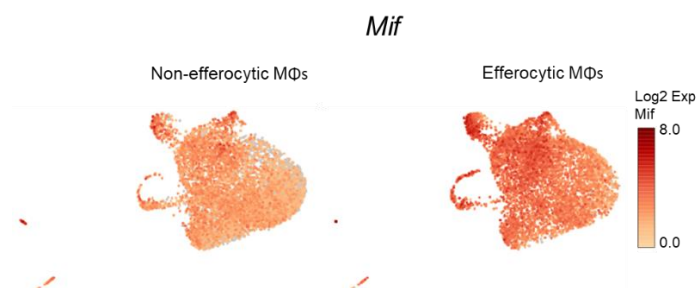
798
799
800
801
802

Figure 2–Figure supplement 2. STAT3 inhibition (S3I-201) in FVB/NJ bone marrow macrophages efferocytosing apoptotic prostate cancer Myc-CaP cells (n=3 per group).



803
804
805
806
807

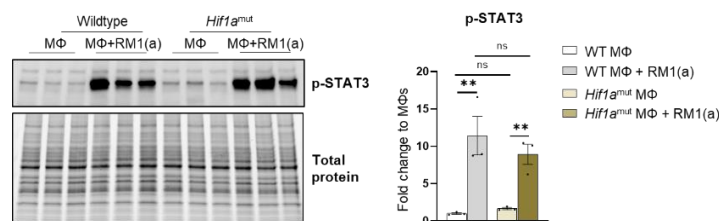
Figure 3–Figure supplement 1. Single-cell plots of *Mif* expression in efferocytic macrophages (corresponding to Exp. 1)



808

809 **Figure 4—Figure supplement 1.** p-STAT3 expression in efferocytic *Hif1a*^{mut} macrophages compared to control macrophages (n=3).

810



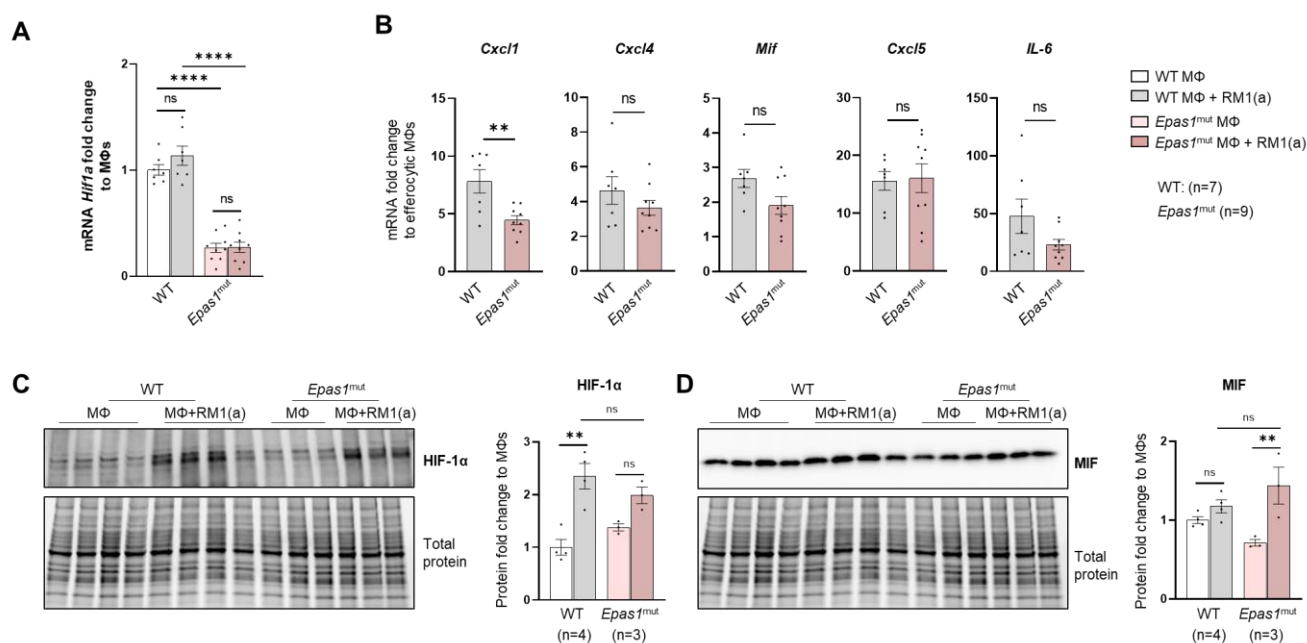
811

812

813

814 **Figure 4—Figure supplement 2.** HIF-2α depletion (*Epas1*^{mut}) effect in efferocytic macrophages.

815

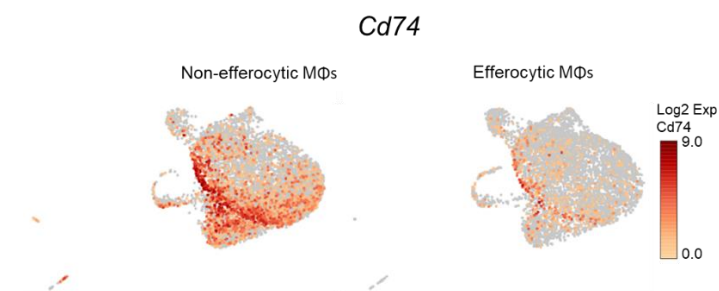


816

817

818 **Figure 6—Figure supplement 1.** Single-cell plots of *Cd74* expression in efferocytic macrophages (corresponding to Exp. 1).

819



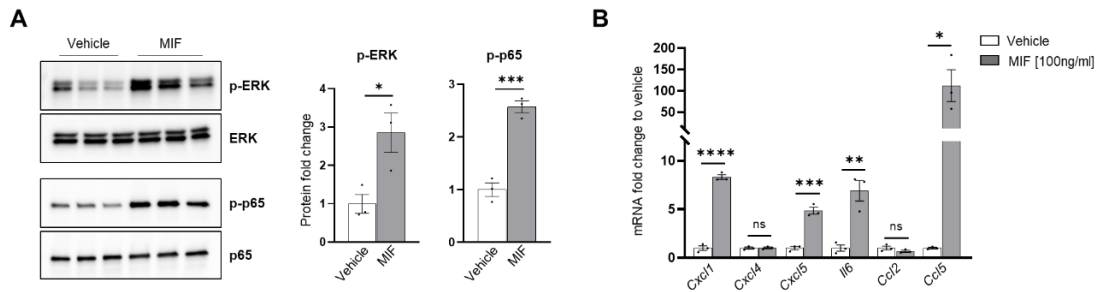
820

821

822

Figure 6—Figure supplement 2. C57BL/6J bone marrow macrophages treatment with MIF (100ng/ml, n=3 per group).

823



824